Output stream of binding neuron with feedback

Alexander Vidybida, Kseniya Kravchuk
Bogolyubov Institute for Theoretical Physics, Kyiv, Ukraine

ABSTRACT

The binding neuron (BN) output firing statistics is considered. The neuron is driven externally by the Poisson stream of intensity λ. The influence of the feedback, which conveys every output impulse to the input with time delay $\Delta \geq 0$, on the statistics of BN's output spikes is considered. The resulting output stream is not Poissonian, and we look for its interspike intervals (ISI) distribution for the case of BN, BN with instantaneous, $\Delta = 0$, and delayed, $\Delta > 0$, feedback. For the BN with threshold 2 an exact mathematical expressions as functions of λ, Δ and BN's internal memory, τ are derived for the ISI distribution, output intensity and ISI coefficient of variation. For higher thresholds these quantities are found numerically. The distributions found for the case of instantaneous feedback include jumps and derivative discontinuities and differ essentially from those obtained for BN without feedback. Statistics of a neuron with delayed feedback has remarkable peculiarities as compared to the case of $\Delta = 0$. ISI distributions, found for delayed feedback, are characterized with jumps, derivative discontinuities and include singularity of Dirac's δ-function type. The obtained ISI coefficient of variation is a unimodal function of input intensity, with the maximum value considerably bigger than unity. It is concluded that delayed feedback presence can radically alter neuronal output firing statistics.

Keywords: binding neuron, delayed feedback, information condensation, interspike intervals distribution, leaky integrate-and-fire neuron, Poisson process.

"Although a neuron requires energy, its main function is to receive signals and to send them out – that is, to handle information."
F. Crick, *The Astonishing Hypothesis*, 1994.

INTRODUCTION

The role of input spikes timing in functioning of either single neuron, or neural net has been addressed many times, as it constitutes one of the main problem in neural coding. The role of timing was observed in processes of perception (MacLeod et al., 1988), memory (Hebb, 1949), objects binding and/or segmentation (Eckhorn, 1988; Engel at al, 1991b; Llinás et al, 1994; Leonards et al, 1996). At the same time, where does the timing come from initially? In reality, some timing can be inherited from the external world during primary sensory reception. In auditory system, this happens for the evident reason that the physical signal, the air pressure time course, itself has pronounced temporal structure in the millisecond time scale, which is retained to a great extent in the inner hair cells output (Cariani, 2001). In olfaction, the physical signal is produced by means of adsorption-desorption of odor molecules, which is driven by Brownian motion. In this case, the primary sensory signal can be represented as Poisson stream, thus not having any remarkable temporal structure. Nevertheless, temporal structure can appear in the output of a neuron fed by a structureless signal. After primary reception, the output of corresponding receptor cells is further processed in primary sensory pathways, and then in higher brain areas. During this processing, statistics of poststimulus spiking activity undergoes substantial transformations, see, e.g.

(Eggermont, 1991). After these transformations, the eventual pattern of activity is far away from the initial one. This process is closely related to the information condensation (König & Krüger, 2006).

We now put a question: What kind of physical mechanisms might underlie these transformations? It seems that, among others, the following features are responsible for spiking statistics of a neuron in a network: (i) several input spikes are necessary for a neuron from a higher brain area to fire an output spike (see, e.g. Andersen et al., 1990; Gerstner & Kistler, 2002); (ii) a neural net has numerous interconnections, which bring about feedback and reverberating dynamics in the net. Due to (i) a neuron must integrate over a time interval in order to gather enough input impulses to fire. As a result, in contrast to Poisson stream, the shortest ISIs between output spikes will no longer be the most probable. Due to reverberation, an individual neuron's

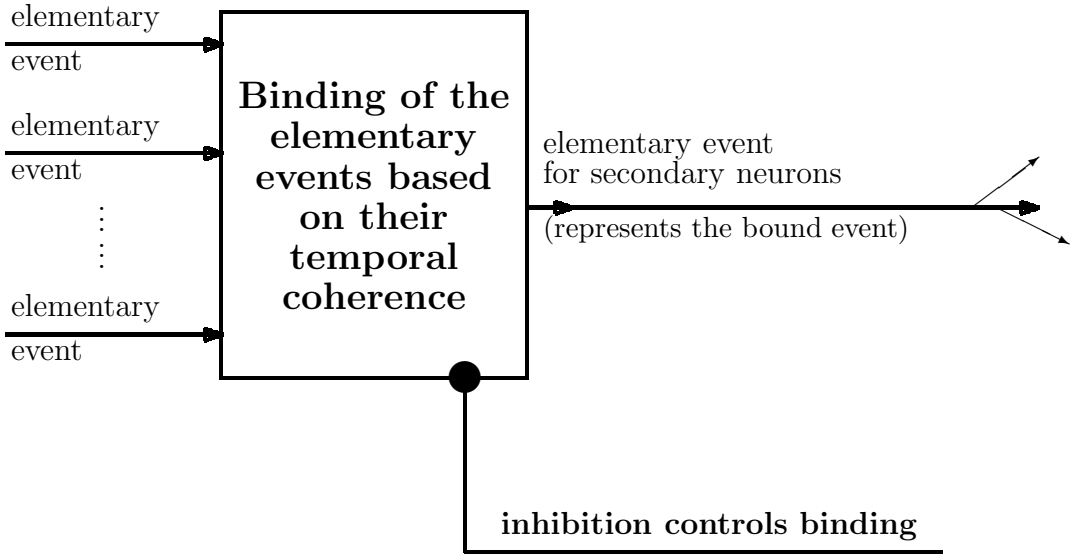

Figure 1. Signal processing in the binding neuron model (Vidybida, 1996a).

output impulses can have some delayed influence on the input of that same neuron. This can be the source of positive feedback which results in establishing of dynamics partially independent of the stimulating input (compare with König & Krüger, 2006; Kistler & De Zeeuw, 2002), and which governs neuronal spiking statistics.

In this text, we consider a simplest possibility to test influence of (i), (ii), above on neuronal firing statistics. As neuronal model we take single binding neuron. Below, we describe the binding neuron (BN) model, as possible abstract concept of signal processing in a generic neuron. Further we obtain exact mathematical expression describing the output firing statistics when BN is fed with input Poisson stream (Vidybida, 2007). The expression obtained is then utilized for describing firing statistics of BN when each output impulse is fed back to the BN's input. Cases of instantaneous (Vidybida, 2008) and delayed feedback are considered. Exact mathematical expressions are derived if BN has threshold 2. For higher thresholds, the firing statistics is calculated numerically, by means of Monte Carlo algorithm. The distributions of interspike intervals found are characterized with discontinuities of jump type, and include singularity of Dirac δ-function type. It is concluded that presence of feedback can radically alter neuronal output firing statistics.

THE BINDING NEURON MODEL

The understanding of mechanisms of higher brain functions expects a continuous reduction from higher activities to lower ones, eventually, to activities in individual neurons, expressed in terms of membrane potentials and ionic currents. While this approach is correct scientifically and desirable for applications, the complete range of the reduction is unavailable to a single researcher/engineer due to human brain

limited capacity. In this connection, it would be helpful to abstract from the rules by which a neuron changes its membrane potentials to rules by which the input impulse signals are processed in the neuron. The “coincidence detector”, and “temporal integrator” are the examples of such an abstraction, see discussion by König et al. (1996).

One more abstraction, the binding neuron (BN) model, is proposed as signal processing unit (Vidybida, 1996b), which can operate either as coincidence detector, or temporal integrator, depending on quantitative characteristics of stimulation applied. This conforms with behavior of real neurons, see, e.g. work by Rudolph & Destexhe (2003). The BN model is inspired by numerical simulation of Hodgkin-Huxley-type neuron stimulated from many synaptic inputs (Vidybida, 1996b). It describes functioning of a neuron in terms of events, which are input and output impulses, and degree of temporal coherence between the input events, see Fig. 1. Mathematically, this can be realized as follows. Each input impulse is stored in the BN for a fixed time, τ. The τ is similar to the “tolerance interval” discussed by MacKay (1962, p. 42). All

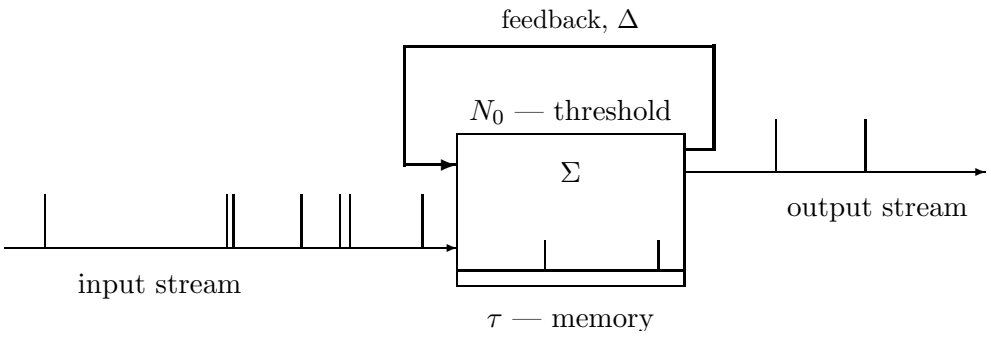

Figure 2. Binding neuron with feedback line under Poisson stimulation. Multiple input lines with Poisson streams are joined into a single one here. Δ is the delay duration in the feedback line.

input lines are excitatory. Slow (potassium-type) inhibition can be introduced by decreasing the value of τ, as it controlls the degree of temporal coherence between input impulses in a compound stimulus, suitable to trigger BN (Vidybida, 1998). The neuron fires an output impulse if the number of stored impulses, Σ, is equal or higher then threshold value, N_0. It is clear, that BN is triggered when a bunch of input impulses is received in a narrow temporal interval. In this case the bunch could be considered as compound event, and the output impulse – as an abstract representation of this compound event. One could treat this mechanism as binding of individual input events into a single output event, provided the input events are coherent in time. Such interpretation is suggested by binding of features/events in largescale neuronal circuits (Eckhorn, 1988; Damasio, 1989; Engel et al., 1991a). The idea, that the output impulse could be considered as abstract representation of the compound input event is closely related to the information condensation, which is observed during neural processing (König & Krüger, 2006).

Formalization of BN functioning

It would be interesting to characterize the BN input-output relations in the form of transfer function, which allows to calculate output in terms of input. In our case input T_{in} is the sequence of arriving moments of standard impulses:

$$T_{in} = \{l_1, l_2, l_3, l_4, ...\}.$$

The output T_{out} is the sequence of firing moments of BN:

$$T_{out} = \{ f_1, f_2, ... \}.$$

It is clear that $T_{out} \subset T_{in}$. The transfer function in our case could be the function $\sigma(l)$, $l \in T_{in}$, which equals 1 if l is the firing moment, $l \in T_{out}$, and 0 otherwise. For BN with threshold N_0 required function can be constructed as follows.

It is clear that first $N_0 - 1$ input impulses are unable to trigger firing, therefore

$$\sigma(l_1) = 0, ..., \sigma(l_{N_0 - 1}) = 0.$$

The next input is able to trigger firing iff all N_0 inputs are coherent in time:

$$\sigma(N_0) = 1, \quad \text{iff} \quad t_{N_0} - t_1 \le \tau.$$

In order to determine $\sigma(l_{N_0 + k})$, $k \ge 1$, one must take into acount all previous input moments, therefore we use notation $\sigma_{T_{in}}$ instead of σ. The values of $\sigma_{T_{in}}(l_{N_0 + k})$ can be determined recursively:

$$\sigma_{T_{in}}(l_{N_0 + k}) = 1, \quad \text{iff} \quad \begin{cases} t_{N_0 + k} - t_{k+1} \le \tau, \\ \sigma_{T_{in}}(l_i) = 0 \quad \text{for all} \quad i \in \{k+1, ..., N_0 + k - 1\}. \end{cases}$$

The function $\sigma_{T_{in}}$ describes completely BN model for arbitrary threshold value $N_0 \ge 2$. For the trivial case $N_0 = 1$, obviously, $\sigma_{T_{in}}(l_i) = 1$ for all $i \ge 1$.

OUTPUT STREAM OF BINDING NEURON WITHOUT FEEDBACK

In this section, we consider BN, which has threshold $N_0 = 2$, internal memory duration τ and is stimulated with Poisson stream in any of its input line (Vidybida, 2007). In this case, multiple input lines shown in Fig. 1 can be replaced with a single one with Poisson stream in it, which has intensity, λ, equal to the sum of intensities in all input lines. This gives schematic presentation of BN as in Fig. 2 with feedback line removed.

Output interspike intervals (ISI) distribution

In order to find firing statistics, one should take into account that BN with threshold 2 emits an output impulse every time when an input impulse is received not later then τ unints of time after its immediate predecessor, and the predecessor itself have not triggered emission of output impulse. The ouput stream statistics can be represented in terms of the probability density for distribution of length of interspike intervals (ISI) in the stream. For this purporse, it is enough to find the probability $P^0(t)dt$ that first output impulse appears t units of time after switching (with precision dt). This output event can be secured due to several alternative input events, which are indexed with the number k of the input impulse, which triggers the output.

It is clear that $2 \le k \le k_{\max}$, where $k_{\max} = \left[t/\tau \right] + 2$ and $[x]$ denotes integral part of x. Let $t_1, t_2, \ldots, t_{k-1}$ denote moments when input impulses are received. Then realisation of the k-th input alternative means that intervals $[0; t_1[$, $]t_1; t_2[, \ldots,]t_{k-1}; t[$ are free of input impulses, and each interval $dt_1, \ldots, dt_{k-1} dt$ in the vicinity of $t_1, t_2, \ldots, t_{k-1}, t$, respectively, has exactly one impulse. By the definition of Poisson process (Gnedenko, 1989), this realisation has the following probability:

$$e^{-\lambda t_1}\lambda dt_1 e^{-\lambda(t_2-t_1)}\lambda dt_2 \ldots e^{-\lambda(t_{k-1}-t_{k-2})}\lambda dt_{k-1} e^{-\lambda(t-t_{k-1})}\lambda dt,$$

and one can calculate the probability $P_k^0(t)\,dt$ of the k-th alternative by integrating the above expression over the domain of coordinates $t_1, t_2, \ldots, t_{k-1}$ defined by the following conditions:

$$t_1 \geq 0, t_1 + \tau < t_2, \ldots, t_i + \tau < t_{i+1}, \ldots, t_{k-2} + \tau < t_{k-1} < t, \tag{1}$$

and $t - t_{k-1} < \tau$. Notice that

$$e^{-\lambda t}\lambda^{k-1} \int_0^{t-(k-2)\tau} dt_1 \int_{t_1+\tau}^{t-(k-3)\tau} dt_2 \ldots \int_{t_{k-2}+\tau}^{t} dt_{k-1}\lambda dt = e^{-\lambda t}\lambda^{k-1}\frac{\left(t-(k-2)\tau\right)^{k-1}}{(k-1)!}\lambda dt. \tag{2}$$

If $k = k_{\max}$, then condition (1) secures that $(k-1)$-th input impulse falls into interval $]t-\tau; t[$, and arrival of k-th impulse at moment t will trigger output impulse. Therefore, in this case

$$P_k^0(t)\,dt = e^{-\lambda t}\lambda^{k-1}\frac{\left(t-(k-2)\tau\right)^{k-1}}{(k-1)!}\lambda dt, \qquad k = k_{\max}.$$

If $k < k_{\max}$, then integral (2) includes configurations with $t_{k-1} < t - \tau$. For those configurations, arrival of k-th input impulse at moment t will not trigger an output. The contribution of such unfavorable configurations in the integral (2) is given by the following expression:

$$e^{-\lambda t}\lambda^{k-1} \int_0^{t-(k-1)\tau} dt_1 \int_{t_1+\tau}^{t-(k-2)\tau} dt_2 \ldots \int_{t_{k-2}+\tau}^{t-\tau} dt_{k-1}\lambda dt = e^{-\lambda t}\lambda^{k-1}\frac{\left(t-(k-1)\tau\right)^{k-1}}{(k-1)!}\lambda dt,$$

which one must subtract from expression (2). Thus for $2 \leq k \leq k_{\max}$ one has:

$$P_k^0(t)\,dt = e^{-\lambda t}\frac{\lambda^{k-1}}{(k-1)!}\left(\left(t-(k-2)\tau\right)^{k-1} - \left(t-(k-1)\tau\right)^{k-1}\right)\lambda dt.$$

The whole probability one finds as sum of probabilities of all alternatives. Notice that $k_{\max}$ is changed by 1 when the value of t crosses a point $m\tau$ with m being a whole number. Thus one can say for $m = 0,1,2,\ldots$: if $m\tau \leq t < (m+1)\tau$, then

$$\begin{aligned} P^0(t)\,dt &= e^{-\lambda t}\frac{\lambda^{m+1}}{(m+1)!}(t-m\tau)^{m+1}\lambda dt + \\ &+ \sum_{2\leq k\leq m+1} e^{-\lambda t}\frac{\lambda^{k-1}}{(k-1)!}\left(\left(t-(k-2)\tau\right)^{k-1} - \left(t-(k-1)\tau\right)^{k-1}\right)\lambda dt. \end{aligned} \tag{3}$$

Eq. (3) can be rewritten as follows:

$$m\tau \leq t < (m+1)\tau \quad \Rightarrow \quad P^0(t) = y_m(t), \quad m = 0,1,\ldots, \tag{4}$$

where $y_i(t)$ are defined according to the following recurrent relation:

$$\begin{aligned} y_i(t) &= y_{i-1}(t) + \frac{\lambda^{i+2}}{(i+1)!}(t-i\tau)^{i+1}e^{-\lambda t} - \frac{\lambda^{i+1}}{i!}(t-i\tau)^{i}e^{-\lambda t}, \\ y_0(t) &= e^{-\lambda t}\lambda^2 t, \quad i = 0,1,\ldots, \quad t > 0. \end{aligned} \tag{5}$$

Let us denote with $\Pi(t)$ the probability to get an output ISI, which is longer than t:

$$\Pi(t) \equiv \int_t^{\infty} P^0(t)\,dt. \tag{6}$$

Taking into acconut (4) and performing integration in (6), one obtains (Vidybida, 2006)

$$\Pi(t) = e^{-\lambda t}\sum_{k=0}^{\left[t/\tau\right]}\frac{\left(\lambda\left(t-\left[\frac{t}{\tau}\right]\tau\right)\right)^{\left[t/\tau\right]+1-k}}{\left(\left[\frac{t}{\tau}\right]+1-k\right)!}\left(1+\sum_{l=1}^{k}\frac{(\lambda\tau)^l(k-l)^l}{l!}\right)+$$
$$+e^{-\lambda t}\left(1+\sum_{l=1}^{\left[t/\tau\right]}\frac{(\lambda\tau)^l\left(\left[\frac{t}{\tau}\right]+1-l\right)^l}{l!}\right). \tag{7}$$

Output intensity

One can define the BN output intensity, or firing rate, λ_o, as inversed of the mean interspike interval, W_1, in the output stream:

$$\lambda_o = \frac{1}{W_1}.$$

W_1 can be calculated based on the exact expression (3):

$$W_1 = \mathrm{E}(W) = \int_0^{\infty} tP^0(t)\,dt = \frac{1}{\lambda}\left(2+\frac{1}{e^{\lambda\tau}-1}\right), \tag{8}$$

which delivers for λ_o

$$\lambda_o = \frac{1-e^{-\lambda\tau}}{2-e^{-\lambda\tau}}\lambda. \tag{9}$$

The output intensity for thresholds 2 and 3 can be calculated without referring to exact expressions for output ISI distributions, see (Vidybida, 2007).

Properties of the ISI distribution

By integrating expression (3) over interval $[0;\infty[$ one can check that the probability density (3) is normalized to 1, as it should be.

The ISI distribution (3) is unimodal, see Fig. 3, a. It can be proven that $P^0(t)$ has maximum at point $t = \min(\tau; 1/\lambda)$. For large t, function $P^0(t)$ decreases exponentially. Namely, for any pair (λ,τ) there exist positive A, α, B, β, such, that for all t large enough the following inequality holds:

$$Be^{-\beta t} < P^0(t) < Ae^{-\alpha t}. \tag{10}$$

Theorem 1.

Output ISI coefficient of variation for single BN under Poisson stimulation ranges between $1/\sqrt{2}$ *and 1 in the case* $N_0 = 2$ *:*

$$\forall\lambda,\tau>0 \quad c_V \in \left]\frac{1}{\sqrt{2}};1\right[.$$

Proof.

Coefficient of variation, c_V, of distribution (3) can be found as follows. By definition

$$c_V = \sqrt{\frac{W_2}{W_1^2} - 1}, \tag{11}$$

where W_1 is given in (8), and W_2 is the second moment:

$$\int_0^\infty t^2 P^0(t)\,dt = \frac{2}{\lambda^2}\frac{3e^{2\lambda\tau} + (\lambda\tau - 3)e^{\lambda\tau} + 1}{\left(e^{\lambda\tau} - 1\right)^2}. \tag{12}$$

Substitute this into (11), which gives

$$c_V = \sqrt{\frac{2\lambda\tau e^{\lambda\tau} + 0.5}{4e^{2\lambda\tau} - 4e^{\lambda\tau} + 1} + \frac{1}{2}}. \tag{13}$$

Since $c_V'(\lambda\tau) < 0$ for all $\lambda, \tau > 0$. The coefficient of variation given in (13) is decreasing function of $\lambda\tau$ with $c_V \to 1$ for $\lambda\tau \to 0$ and $c_V \to 1/\sqrt{2}$ for $\lambda\tau \to \infty$. The graph of $c_V(\lambda\tau)$ is given in Fig. 7, a. Theorem 1 is proven.

Theorem 2.

Output ISI of binding neuron under Poisson stimulation are independent of eachother.

Proof.

Since just after firing the BN appears in the unique standard state (empty neuron), the conditional probability $P(t_2 \mid t_1)\,dt_2$ to obtain an output ISI of duration t_2, with precision dt_2, provided the previous one had duration t_1, equals $P^0(t_2)\,dt_2$. This exactly proves Theorem 2.

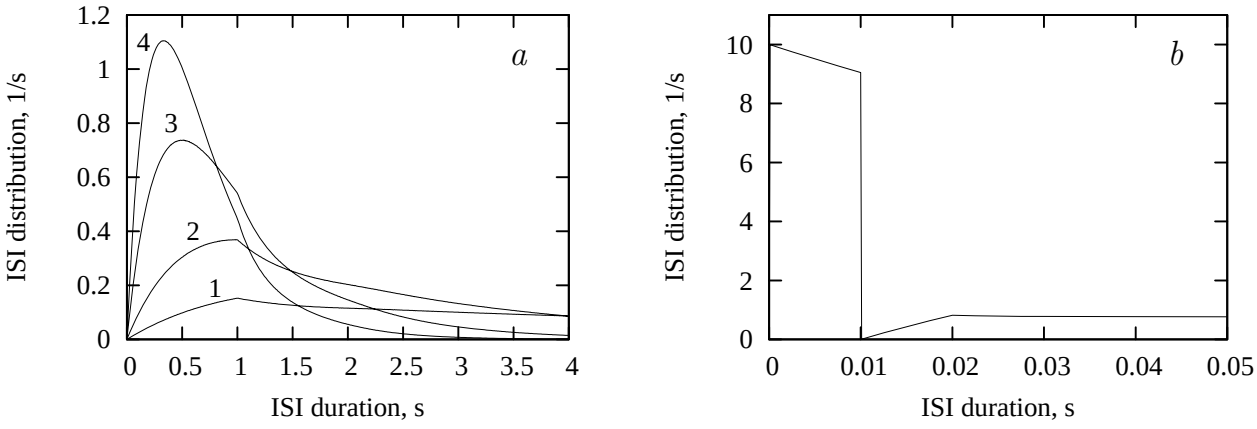

Figure 3. ISI distributions for BN without feedback (a) and with instantaneous feedback (b).
a: $P^0(t)$ for τ =1 s, $N_0 = 2$, calculated in accordance with (3).
Curves 1, 2, 3, 4 correspond to λ = 0.5 s^{-1}, 1 s^{-1}, 2 s^{-1}, 3 s^{-1};
b: $P_f(t)$ for τ = 10 ms, λ = 10 s^{-1}, $N_0 = 2$, calculated in accordance with (15);.

BINDING NEURON WITH INSTANTANEOUS FEEDBACK (BNF)

Let us assume that each output impulse of BN with Poisson stimulation is immediately fed back into BN's input. This gives BN with instantaneous feedback, Fig. 2 with $\Delta = 0$ (Vidybida, 2008).

Firing statistics of this construction can be found utilizing results obtained for BN without feedback.

Output Intensity of BNF with Threshold 2

Let us expect that the output stochastic process is stationary. This can be achived if a long period of time has been passed after switching. In this case one can define/calculate the output intensity, λ_o, as the factor in the expression $\lambda_o dt$, which gives the probability to obtain an output impulse in the infinitesimal interval dt, if nothing is known about previous states of the neuron.

The probability to obtain an output impulse from the BNF with threshold 2 in the interval $[t;t+dt[$, $\lambda_o dt$, can be calculated as product of probabilities of two independent events: (i) an input impulse, I_1, arrives in the interval $[t-\tau;t[$; (ii) the next input impulse, I_2, arrives in the interval $[t;t+dt[$. Event (ii) has probability λdt. Event (i) has the same probability as having in Poisson stream two successive events (here I_1, I_2) separated by time interval, which is shorter than τ. This probability is $1-e^{-\lambda\tau}$. Thus,

$$\lambda_o = \left(1-e^{-\lambda\tau}\right)\lambda. \qquad (14)$$

Interesting, that for high input rates ($\lambda \to \infty$), the triggering rate becomes equal to the input one. This can be explained as follows. If input rate is very high, almost all input ISIs become shorter then τ. In this case, any input, stored in the BNF will eventually give rise to output spike, which is immediately used as input for empty neuron due to feedback. This effectively doubles the input rate. Namely, any input impulse triggers the BNF, and then it is applied to empty BNF through feedback. As a result, the output stream for high λ literally reproduces the input one: any input spike becomes the output one without delay. This same reasoning allows one to say that output rate of BNF with any threshold N_0 approaches $\lambda/(N_0-1)$ when $\lambda \to \infty$. Compare this with BN without feedback, where corresponding limit output rate is λ/N_0.

Another way to define λ_o is to use instantaneous intensity (Khinchin, 1955), $\lambda_o(t)$, which is the probability to obtain an output impulse at moment t in infinitesimal interval s divided by s:

$$\lambda_o(t) = \lim_{s\to 0}\frac{w(s,t)}{s},$$

where $w(s,t)$ denotes the probability to obtain impulse in the interval $[t;t+s[$. As λ_o one can choose the following

$$\lambda_o = \lim_{t\to\infty}\lambda_o(t).$$

It can be shown that this definition brings about the same value for λ_o as is given in Eq. (14). Calculations based on this definition can be fulfilled with the help of Theorem of §8, Part XI in (Feller, 1966).

Distribution of Output Intervals for BNF with $N_0 = 2$

Consider the ISI distribution for binding neuron with instantaneous feedback, $P_f(t)$.

Theorem 3.
For binding neuron with $N_0 = 2$ and instantaneous feedback under Poisson stimulation the following holds:

$$\begin{cases} 0 \le t < \tau \;\Rightarrow\; P_f(t) = e^{-\lambda t}\lambda, \\ \tau \le t \;\Rightarrow\; P_f(t) = e^{-\lambda\tau}P^0(t-\tau). \end{cases} \tag{15}$$

Proof.
The ISI length t, where $t < \tau$, can be obtained provided the first input impulse arrives not later then τ units of time after the previous firing. In this case, the neuron still keeps impulse received from the previous firing through the feedback line, and the input secures the threshold to be achieved and BNF to fire. There is no other way to get output interval t shorter then τ. Thus, for $t \in [0;\tau[$, the probability density distribution of ISI coincides with the distribution for the input Poisson stream:

$$P_f(t)\,dt = e^{-\lambda t}\lambda\,dt, \quad t \in [0;\tau[.$$

ISI duration t, where $t > \tau$, means that impulse from the feedback line does not contribute into firing, since it was lost at moment τ after previous firing. From that moment, the BNF works like BN without feedback and is triggered at moment t with probability $P^0(t-\tau)$. In order to obtain probability of t one should multiply this probability with the probability to have interval longer than τ in the input Poisson stream. This gives:

$$P_f(t) = e^{-\lambda\tau}P^0(t-\tau), \quad t \ge \tau.$$

Theorem 3 is proven.

Function $P_f(t)$ can also be calculated from the first principles (Vidybida, 2008).

Properties of the distribution

The expression (15) together with the fact that $P^0(t)$ is normalized, allows one to check easily that $P_f(t)$ is normalized as well:

$$\int_0^\infty P_f(t)\,dt = 1.$$

It is clear from (15) that $P_f(t)$ satisfies asymptotic condition like (10), but is discontinuous at point $t = \tau$. The graph of $P_f(t)$ is shown in Fig. 3, b.

Having for $P_f(t)$ representation (15), one can easily calculate mean interspike interval, W_1 (Vidybida, 2008):

$$W_1 = \int_0^\infty tP_f(t)\,dt = \frac{1}{\lambda\left(1-e^{-\lambda\tau}\right)}.$$

Notice, that as expected for the stationary point process, mean output ISI is reversed output intensity given in (14).

Theorem 4.

Output ISI coefficient of variation for BN with instantaneous feedback under Poisson stimulation exceeds unity for any input intensity and BN's memory duration in the case $N_0 = 2$ *:*

$\forall \lambda, \tau > 0 \;\; c_V > 1$.

Proof.

In order to prove Theorem 2 consider the second moment W_2 of distribution (15) (Vidybida, 2008):

$$W_2 = \int_0^\infty t^2 P_f(t)\, dt = \frac{2e^{\lambda\tau}}{\lambda^2} \frac{e^{\lambda\tau} + \lambda\tau}{\left(e^{\lambda\tau} - 1\right)^2}.$$

Substituting this into definition (11), one gets:

$$c_V = \sqrt{2\lambda\tau e^{-\lambda\tau} + 1}. \qquad (16)$$

Coefficient of variation, given in (16), increases monotonically from $c_V = 1$ at $\lambda\tau = 0$ to its maximum value, $c_{V\max}$,

$$c_{V\max} = \sqrt{2e^{-1} + 1} \approx 1.32$$

at $\lambda\tau = 1$, and then gradually decreases to its asymptotic value $c_V \to 1$ when $\lambda\tau \to \infty$ (Fig. 7, b). Therefore, for any finite $\lambda\tau > 0$ one obtains $c_V > 1$. Theorem 4 is proven.

Theorem 5.

Output ISI of binding neuron with instantaneous feedback under Poisson stimulation are independent of eachother.

Proof.

Since just after firing the neuron starts from standard state (keeps a single impulse with time to live equal τ), the conditional probability $P(t_2 \mid t_1)\, dt_2$ to obtain an output ISI of duration t_2, with precision dt_2, provided the previous one had duration t_1, equals $P_f(t_2)\, dt_2$. This exactly proves Theorem 5.

This fact depends crucially on the immediateness of feedback.

BINDING NEURON WITH DELAYED FEEDBACK

Let us assume that each output impulse of BN with Poisson stimulation is fed back into BN's input with delay $\Delta > 0$. This gives BN with delayed feedback, Fig. 2. Firing statistics of this construction can be found utilizing results obtained for BN without feedback.

Any output impulse of BN with feedback line may be produced either with impulse from the line involved, or not. We assume that, just after firing and sending output impulse, the line is never empty. This assumption is selfevident for output impulses produced without impulse from the line, or if the impulse from the line was involved, but entered empty neuron. In the letter case, the second (triggering) impulse comes from the Poisson stream, neuron fires and output impulse goes out as well as enters the empty line. On the other hand, if impulse from the line triggers BN, which already keeps one impulse from the input stream, it may be questionable if the output impulse is able to enter the line, which was just filled with the impulse. We expect it does. This means biologically that we ignore the refraction time - a

short period necessary for a nervous fibre to recover from conducting previous spike before it is able to serve for the next one. Thus, at the beginning of any output ISI, the line keeps impulse with time to live s, where $s \in]0;\Delta]$.

For analytical calculations we consider threshold value $N_0 = 2$.

Calculations

In previous sections, the output stream statistics of BN (with feedback line removed, $\Delta = \infty$) and BN with instantaneous feedback ($\Delta = 0$) was considered. In both cases, at the beginning of every output ISI BN starts from the standard state, which keeps no information about previous events. On the contrary, the state of BN with delayed feedback is characterized by additional parameter, s, which gets no standard value at the beginning of output ISI and depends on previous events. In other words, in this case two sorts of random variability should be taken into account, namely, the variability of driving Poisson process and the variability in the state of the feedback line at the beginning of output ISI[i].

The main idea is to restrict ourselves first to the imaginary case of fixed s, taking into account only variability of the input Poisson stream, and then to account the variability of s. For this purpose we introduce conditional probability density $P^{\Delta}(t \mid s)$, corresponding to fixed s. Namely, $P^{\Delta}(t \mid s)dt$ gives the probability to obtain an output ISI in interval $[t;t+dt[$, if at the beginning of this ISI there was an impulse in the feedback line with time to live equal s. Once it is found, the output ISI distribution $P^{\Delta}(t)$ can be calculated as

$$P^{\Delta}(t) = \int_0^{\Delta} P^{\Delta}(t \mid s)\, f(s)\, ds, \tag{17}$$

where $f(s)$ denotes stationary distribution for time to live $s \in]0;\Delta]$ of impulse in the feedback line at the beginning of output ISI. Function $f(s)$ keeps no information about the state of the system at the moment it was switched on.

Such stationary distribution $f(s)$ must satisfy the following balance equation:

$$\int_0^{\Delta} P(s_2 \mid s_1)\, f(s_1)\, ds_1 = f(s_2), \tag{18}$$

where $P(s_2 \mid s_1)$, multiplied by ds_2, gives the probability to have at the beginning of an ISI the impulse in the feedback line with time to live equal s_2, with precision ds_2, if at the beginning of the previous ISI there was an impulse with time to live equal s_1.

So, in order to find output ISI distribution $P^{\Delta}(t)$ one should derive exact expressions for $P^{\Delta}(t \mid s)$, $P(s_2 \mid s_1)$ and $f(s)$ first.

Conditional probability distribution $P^{\Delta}(t \mid s)$

The explicit expression for conditional probability distribution $P^{\Delta}(t \mid s)$ depends on the domain, t belongs to. Basic domains for $P^{\Delta}(t \mid s)$ are shown in Fig. 4, a.

Consider case C1, where $t < s$. The impulse is still passing the feedback line, thus having no influence on BN's statistics, which gives the following

$$P^{\Delta}(t \mid s) = P^{0}(t), \quad t < s. \tag{19}$$

Here $P^{0}(t)$ denotes ISI distribution for BN without feedback, determined by Eq. (3).

Consider case C2. The probability to obtain output impulse exactly througt the time s after the last one is not infinitesimally small. This event is equivalent to the event $A_{S_1}(s)$ that BN starts empty at moment 0 and appears without triggerings in state S_1 (keeps impulse) at moment s. In order to obtain the probability $P\{A_{S_1}(s)\}$, let us take into account that $P^{0}(s)ds$ can be obtained as the product of $P\{A_{S_1}(s)\}$ and the probability to get input impulse in infinitesimal interval ds, which is λds. Therefore,

$$P\{A_{S_1}(s)\} = \frac{P^{0}(s)}{\lambda}, \tag{20}$$

and

$$P^{\Delta}(t \mid s) = \frac{P^{0}(s)}{\lambda} \cdot \delta(t-s), \quad t \in]s-\varepsilon; s+\varepsilon[. \tag{21}$$

To obtain ISI from the range $s < t < s+\tau$, case C3, the following events must happen: i) impulse from the feedback line, arriving at the moment s, doesn't trigger BN; ii) interval $]s;t[$ is free from input impulses and the first one arrives within interval $[t;t+dt[$. As the BN is driven by the Poisson stream, events i) and ii) are mutually independent.

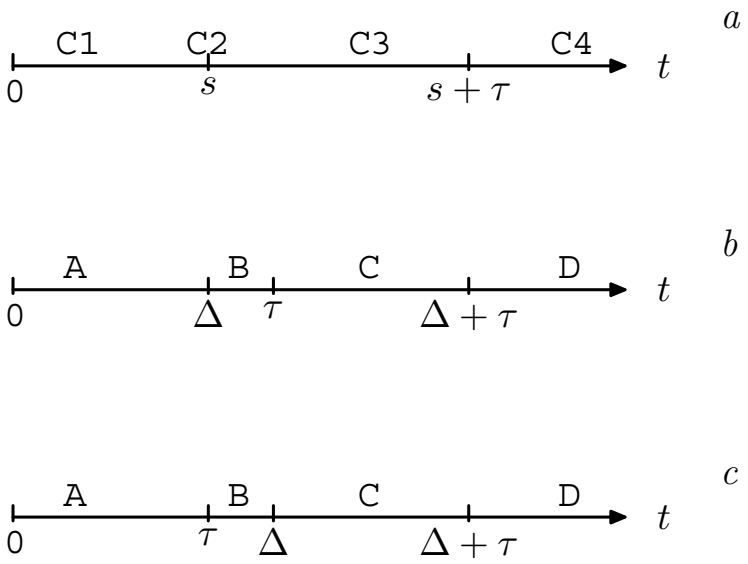

Figure 4. Domains of t used for calculating conditional probability $P^{\Delta}(t \mid s)$ (a), ISI distribution $P^{\Delta}(t)$ for the cases $\Delta < \tau$ (b) and $\Delta \geq \tau$ (c).

Event i) is equivalent to event $A_{S_0}(s)$ that BN starts empty at moment 0 and appears without triggerings in state S_0 (keeps no impulses) at moment s. In order to find its probability $P\{A_{S_0}(s)\}$ one

should take into account that at any moment s BN either appears without triggering in the state S_0 or S_1, or it has already fired a spike. Thus,

$$P\left\{A_{S_0}(s)\right\} = 1 - P\left\{A_{S_1}(s)\right\} - \left(1 - \Pi(s)\right) = \Pi(s) - \frac{P^0(s)}{\lambda}, \tag{22}$$

where $\Pi(t)$ denotes the probability to obtain ISI longer then t at the output of BN without feedback, and is given in (7).

The probability of ii) is $e^{-\lambda(t-s)}\lambda dt$, which allows one to obtain

$$P^{\Delta}(t \mid s) = e^{-\lambda(t-s)}\left(\lambda\Pi(s) - P^0(s)\right), \quad t \in]s; s+\tau[. \tag{23}$$

In the case C4, $t \geq s+\tau$. Such output ISI requires several independent events to happen: i) $A_{S_0}(s)$; ii) interval $]s; s+\tau[$ is free from input Poissonian impulses; iii) BN without feedback, which starts empty at the moment $s+\tau$, fires for the first time during interval $[t; t+dt[$. The probability of iii) is $P^0(t-s-\tau)dt$. Therefore, taking into account Eq. (22)

$$P^{\Delta}(t \mid s) = \frac{1}{\lambda}e^{-\lambda\tau}\left(\lambda\Pi(s) - P^0(s)\right)P^0(t-s-\tau), \quad t \geq s+\tau. \tag{24}$$

Finally, taking into account Eqs. (19), (21), (23) and (24), one obtains $P^{\Delta}(t \mid s)$ as a sum of singular and regular parts:

$$P^{\Delta}(t \mid s) = P^{\text{sing}}(t \mid s) + P^{\text{reg}}(t \mid s), \tag{25}$$

where

$$P^{\text{sing}}(t \mid s) = \frac{P^0(s)}{\lambda} \cdot \delta(t-s), \tag{26}$$

$$P^{\text{reg}}(t \mid s) = \begin{cases} P^0(t), & \text{t} \in]0;\text{s}], \\ e^{-\lambda(t-s)}\left(\lambda\Pi(s) - P^0(s)\right), & t \in]s; s+\tau], \\ \frac{1}{\lambda}e^{-\lambda\tau}\left(\lambda\Pi(s) - P^0(s)\right)P^0(t-s-\tau), & \text{s}+\tau \leq \text{t}. \end{cases} \tag{27}$$

It can be seen easily from (6) that function $P^{\Delta}(t \mid s)$ is normalized: $\int_0^{\infty} P^{\Delta}(t \mid s)\,dt = 1$.

In particular case of $\Delta < \tau$ one obtains

$$P^{\text{sing}}(t \mid s) = e^{-\lambda s}\lambda s \cdot \delta(t-s), \tag{28}$$

$$P^{\text{reg}}(t \mid s) = \begin{cases} \lambda^2 t e^{-\lambda t}, & \text{t} \in]0;\text{s}], \\ \lambda e^{-\lambda t}, & t \in]s; s+\tau], \\ e^{-\lambda(s+\tau)}P^0(t-s-\tau), & \text{s}+\tau \leq \text{t}, \end{cases} \qquad \text{when} \quad \left[\Delta/\tau\right] = 0. \tag{29}$$

Conditional probabilities $P(s_2 \mid s_1)$

In order to find conditional probabilities $P(s_2 \mid s_1)$, let us first consider the case $s_2 < s_1$. It means that impulse "2" was caused by external input stream, without involvement of feedbacked impulse. Therefore, $P(s_2 \mid s_1)$ coincides with $P^0(t_1)$, where $t_1 = s_1 - s_2$ denotes the first ISI duration:

$$P(s_2 \mid s_1) = P^0(s_1 - s_2), \quad s_2 < s_1 \in]0;\Delta]. \tag{30}$$

If the impulse leaved feedback line during first ISI, the next one will start with $s_2 = \Delta$. Any output ISI, longer than s_1, will contribute to such result. So, one obtains in $P(s_2 \mid s_1)$ the δ-function term with the mass $\Pi(s_1)$:

$$P(s_2 \mid s_1) = \Pi(s_1) \cdot \delta(s_2 - \Delta), \quad s_2 \in]\Delta - \varepsilon;\Delta]. \tag{31}$$

Finally, conditional probability $P(s_2 \mid s_1)$ can be written as follows:

$$\begin{gathered} P(s_2 \mid s_1) = P^{\text{sing}}(s_2 \mid s_1) + P^{\text{reg}}(s_2 \mid s_1), \\ P^{\text{sing}}(s_2 \mid s_1) = \Pi(s_1) \cdot \delta(s_2 - \Delta), \\ P^{\text{reg}}(s_2 \mid s_1) = \begin{cases} P^0(s_1 - s_2), & s_2 < s_1 \in]0;\Delta], \\ 0, & s_2 \geq s_1. \end{cases} \end{gathered} \tag{32}$$

It is clear that function $P(s_2 \mid s_1)$ is also normalized: $\int_0^\Delta P(s_2 \mid s_1)\, ds_2 = 1$.

In particular case $\Delta < \tau$ one obtains:

$$\begin{gathered} P^{\text{sing}}(s_2 \mid s_1) = (\lambda s_1 + 1) e^{-\lambda s_1} \cdot \delta(s_2 - \Delta), \\ P^{\text{reg}}(s_2 \mid s_1) = \begin{cases} e^{-\lambda(s_1 - s_2)} \lambda^2 (s_1 - s_2), & s_2 < s_1 \in]0;\Delta], \\ 0, & s_2 \geq s_1. \end{cases} \end{gathered} \tag{33}$$

Delays distribution $f(s)$

In order to find delays distribution $f(s)$, we first represent it as follows:

$$f(s) = a\delta(s - \Delta) + g(s) = a\delta(s - \Delta) + e^{\lambda s}\varphi(s), \tag{34}$$

where a is a dimentionless constant, $g(s)$ and $\varphi(s)$ – unknown functions, vanishing out of interval $]0;\Delta]$. Substituting Eqs. (32) and (34) to (18) and separating terms without δ-function, one obtains

$$aP^0(\Delta - s_2) + \int_{s_2}^{\Delta} P^0(s_1 - s_2)\, g(s_1)\, ds_1 = g(s_2), \tag{35}$$

or, taking into account (3),

$$ae^{-\lambda\Delta}\left(\sum_{k=1}^{m_{\Delta-s_2}+1}\frac{\lambda^{k+1}}{k!}\left(\Delta-s_2-(k-1)\tau\right)^k-\sum_{k=1}^{m_{\Delta-s_2}}\frac{\lambda^{k+1}}{k!}\left(\Delta-s_2-k\tau\right)^k\right)+$$
$$+\int_{s_2}^{\Delta}\left(\sum_{k=1}^{m_{s_1-s_2}+1}\frac{\lambda^{k+1}}{k!}\left(s_1-s_2-(k-1)\tau\right)^k-\sum_{k=1}^{m_{s_1-s_2}}\frac{\lambda^{k+1}}{k!}\left(s_1-s_2-k\tau\right)^k\right)\varphi(s_1)\,ds_1=\varphi(s_2), \tag{36}$$

where $m_{\Delta-s_2}$, $m_{s_1-s_2}$ denote $\left[\frac{\Delta-s_2}{\tau}\right]$ and $\left[\frac{s_1-s_2}{\tau}\right]$ respectively. Obviously, $m_{s_1-s_2}$ in (36) gets integer values from the range $0,1,\ldots,m_{\Delta-s_2}$, and $m_{\Delta-s_2}$ ranges from 0 to $m_\Delta\equiv\left[\frac{\Delta}{\tau}\right]$.

We put $m_{\Delta-s_2}$ fixed in Eq. (36). It means, that function $\varphi(s)$ and the equation it satisfies should be considered separately at different domains of s:

$$\varphi^0(s)\equiv\varphi(s),\quad s\in]0;\delta[,$$
$$\varphi^j(s)\equiv\varphi(s),\quad s\in[\delta+(j-1)\tau;\delta+j\tau[,\quad j=1,2,\ldots,m_\Delta,$$

where

$$\delta=\Delta-m_\Delta\tau.$$

If first case is assigned with the value $j=0$, $m_{\Delta-s}$ within j-th domain can be found as

$$m_{\Delta-s}=m_\Delta-j. \tag{37}$$

In terms of $\varphi^j(s)$ equation Eq. (36) turns into:

$$ae^{-\lambda\Delta}\left(\sum_{k=1}^{m_\Delta-j+1}\frac{\lambda^{k+1}}{k!}\left(\Delta-s_2-(k-1)\tau\right)^k-\sum_{k=1}^{m_\Delta-j}\frac{\lambda^{k+1}}{k!}\left(\Delta-s_2-k\tau\right)^k\right)+$$
$$+\sum_{n=0}^{m_\Delta-j-1}\int_{\delta+(j+n)\tau}^{s_2+(n+1)\tau}\left(\sum_{k=1}^{n+1}\frac{\lambda^{k+1}}{k!}\left(s_1-s_2-(k-1)\tau\right)^k-\sum_{k=1}^{n}\frac{\lambda^{k+1}}{k!}\left(s_1-s_2-k\tau\right)^k\right)\varphi^{j+n+1}(s_1)\,ds_1+$$
$$+\sum_{n=0}^{m_\Delta-j-1}\int_{s_2+(n+1)\tau}^{\delta+(j+n+1)\tau}\left(\sum_{k=1}^{n+2}\frac{\lambda^{k+1}}{k!}\left(s_1-s_2-(k-1)\tau\right)^k-\sum_{k=1}^{n+1}\frac{\lambda^{k+1}}{k!}\left(s_1-s_2-k\tau\right)^k\right)\varphi^{j+n+1}(s_1)\,ds_1+ \tag{38}$$
$$+\int_{s_2}^{\delta+j\tau}\lambda^2(s_1-s_2)\varphi^j(s_1)\,ds_1=\varphi^j(s_2).$$

Differentiating (38) twice with respect to s_2, one obtains the second-order differential equation for $\varphi^j(s)$:

$$\frac{d^2\varphi^j(s)}{ds^2}-\lambda^2\varphi^j(s)=\Phi^j(s), \tag{39}$$

where

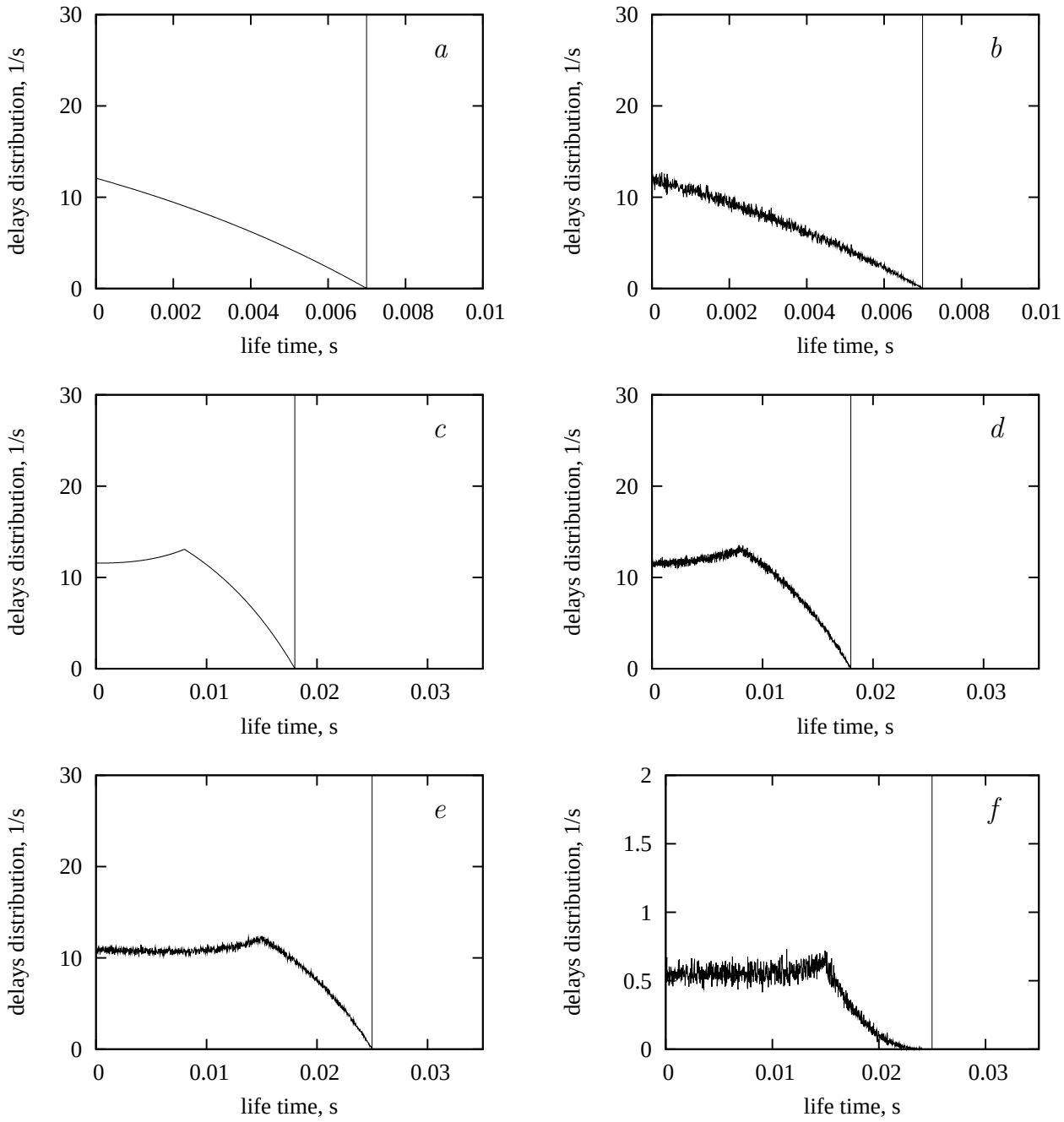

Figure 5. Examples of delays distribution $f(s)$*, obtained analytically (a,c) in accordance with Eqs. (34), (44) – (47), and found numerically by means of Monte Carlo method after 10 000 000 triggerings (b,d,e,f).*

a: $N_0 = 2$, τ *=10 ms,* Δ *=7 ms,* λ *=50* s^{-1}*; b: same parameters as in a;*

c: $N_0 = 2$, τ *=10 ms,* Δ *=18 ms,* λ *=50* s^{-1}*; d: same parameters as in c;*

e: $N_0 = 2$, τ *=10 ms,* Δ *=25 ms,* λ *=50* s^{-1}*; f:* $N_0 = 4$, τ *=10 ms,* Δ *=25 ms,* λ *=50* s^{-1}.

Curves calculated analytically fit perfectly with those found numerically for the same parameters.

$$\Phi^j(s)=ae^{-\lambda\Delta}\left(\sum_{k=2}^{m_\Delta-j+1}\frac{\lambda^{k+1}}{(k-2)!}\left(\Delta-s-(k-1)\tau\right)^{k-2}-\sum_{k=2}^{m_\Delta-j}\frac{\lambda^{k+1}}{k!}\left(\Delta-s-k\tau\right)^{k-2}\right)+$$
$$+\sum_{n=0}^{m_\Delta-j-1}\left(\sum_{k=2}^{n+1}\frac{\lambda^{k+1}}{(k-2)!}\int_{\delta+(j+n)\tau}^{\delta+(j+n+1)\tau}\left(s'-s-(k-1)\tau\right)^{k-2}\varphi^{j+n+1}(s')\,ds'-\right.$$
$$-\sum_{k=2}^{n}\frac{\lambda^{k+1}}{(k-2)!}\int_{\delta+(j+n)\tau}^{\delta+(j+n+1)\tau}\left(s'-s-k\tau\right)^{k-2}\varphi^{j+n+1}(s')\,ds'+ \tag{40}$$
$$\left.+\frac{\lambda^{n+3}}{n!}\int_{s+(n+1)\tau}^{\delta+(j+n+1)\tau}\left(s'-s-(n+1)\tau\right)^{n}\varphi^{j+n+1}(s')\,ds'\right)-\lambda^2\cdot\varphi^{j+1}(s+\tau)-$$
$$-\sum_{n=1}^{m_\Delta-j-1}\frac{\lambda^{n+2}}{(n-1)!}\int_{s+(n+1)\tau}^{\delta+(j+n+1)\tau}\left(s'-s-(n+1)\tau\right)^{n-1}\varphi^{j+n+1}(s')\,ds'.$$

So, the system of $m_\Delta+1$ second-order differential equations for $\varphi^j(s)$ was obtained:

$$\begin{cases}\dfrac{d^2\varphi^{m_\Delta}(s)}{ds^2}-\lambda^2\varphi^{m_\Delta}(s)=0,\\ \dfrac{d^2\varphi^{m_\Delta-1}(s)}{ds^2}-\lambda^2\varphi^{m_\Delta-1}(s)=a\lambda^3e^{-\lambda\Delta}-\lambda^2\varphi^{m_\Delta}(s+\tau)+\lambda^3\int_{s+\tau}^{\Delta}\varphi^{m_\Delta}(s')\,ds',\\ \ldots,\\ \dfrac{d^2\varphi^{j}(s)}{ds^2}-\lambda^2\varphi^{j}(s)=\Phi^j(s),\\ \ldots,\\ \dfrac{d^2\varphi^{0}(s)}{ds^2}-\lambda^2\varphi^{0}(s)=\Phi^0(s).\end{cases} \tag{41}$$

It can be seen from Eq. (40), that system (41) of differential equations has recurrent structure. In order to solve it, one should consider domains with j decreasing from $j=m_\Delta$ to $j=0$ consequently. The solution for j-th domain is then

$$\varphi^j(s)=e^{\lambda s}\left(\frac{1}{2\lambda}\int_{\delta+(j-1)\tau}^{s}e^{-\lambda s'}\Phi^j(s')\,ds'+D_1^j\right)+e^{-\lambda s}\left(-\frac{1}{2\lambda}\int_{\delta+(j-1)\tau}^{s}e^{\lambda s'}\Phi^j(s')\,ds'+D_2^j\right),$$
$$s\in\left[\delta+(j-1)\tau;\delta+j\tau\right[,\quad j=1,2,\ldots,m_\Delta, \tag{42}$$
$$\varphi^0(s)=e^{\lambda s}\left(\frac{1}{2\lambda}\int_{0}^{s}e^{-\lambda s'}\Phi^0(s')\,ds'+D_1^0\right)+e^{-\lambda s}\left(-\frac{1}{2\lambda}\int_{0}^{s}e^{\lambda s'}\Phi^0(s')\,ds'+D_2^0\right),\quad s\in\left]0;\delta\right[,$$

where D_1^j and D_2^j denote unknown constants of integration. In order to find D_1^j and D_2^j as functions of λ, τ, Δ, one should substitute (42) to Eq. (36) and separate terms with different power of s.

For example, when $j=m_\Delta$, one obtains $\varphi^{m_\Delta}(s)=\dfrac{a\lambda e^{-\lambda s}}{2}\left(1-e^{-2\lambda(\Delta-s)}\right)$.

Constant a in (34) is then found from the normalization condition:

$$a+\int_0^{\Delta} g(s)\,ds=1. \tag{43}$$

In particular case of $\Delta<\tau$ there exists single domain for s, namely $s\in\left]0;\delta\right]=\left]0;\Delta\right]$. For $\varphi(s)$ one obtains:

$$\varphi(s)=\frac{a\lambda e^{-\lambda s}}{2}\left(1-e^{-2\lambda(\Delta-s)}\right),\quad s\in\left]0;\Delta\right], \tag{44}$$

$$a=\frac{4e^{2\lambda\Delta}}{(3+2\lambda\Delta)e^{2\lambda\Delta}+1}. \tag{45}$$

The simplest case of $\Delta>\tau$ is realized when $\Delta\in\left[\tau;2\tau\right[$. Two domains should be considered here: $s\in\left]0;\Delta-\tau\right]$ and $s\in\left]\Delta-\tau;\Delta\right]$. Solving (41) for $m_{\Delta}=1$, one obtains

$$\begin{gathered}\varphi^0(s)=\frac{a\lambda}{2}e^{-2\lambda\Delta+\lambda\tau}\left(\lambda s-\lambda(\Delta-\tau)+\frac{1}{2}-e^{-\lambda\tau}\right)\cdot e^{\lambda s}+\frac{a\lambda}{2}\left(-\frac{1}{2}e^{-\lambda\tau}+1\right)\cdot e^{-\lambda s},\quad s\in\left]0;\Delta-\tau\right],\\ \varphi^1(s)=\frac{a\lambda e^{-\lambda s}}{2}\left(1-e^{-2\lambda(\Delta-s)}\right),\quad s\in\left]\Delta-\tau;\Delta\right].\end{gathered} \tag{46}$$

Substituting (46) to the normalization condition (43), one obtains

$$a=\frac{4e^{2\lambda\Delta}}{(3+2\lambda\tau)e^{2\lambda\Delta}+1+\lambda(\Delta-\tau)e^{\lambda\tau}-\lambda(\Delta-\tau)e^{2\lambda\Delta-\lambda\tau}+2\lambda(\Delta-\tau)e^{2\lambda\Delta}}. \tag{47}$$

Graphs of $f(s)$ corresponding to the cases $\Delta<\tau$ and $\Delta\in\left[\tau;2\tau\right[$ are shown at Fig. 5, a – d.

ISI distribution for $\Delta<\tau$

For calculating $P^{\Delta}(t)$ substitute (28), (29) and (34) into Eq. (17). This gives

$$P^{\Delta}(t)=e^{-\lambda t}\lambda t\cdot a\delta(t-\Delta)+e^{-\lambda t}\lambda t g(t)+aP^{\mathrm{reg}}(t\mid\Delta)+\int_0^{\Delta}P^{\mathrm{reg}}(t\mid s)\,g(s)\,ds. \tag{48}$$

Further transformation of (48) depends on the domain, t belongs to. Basic domains of t for the case $\Delta<\tau$ are shown in Fig. 4, b.

Consider case A. Here integration domain, $s\in\left]0;\Delta\right]$, should be splitted into two with point $s=t$. This gives

$$P^{\Delta}(t)=e^{-\lambda t}\lambda t g(t)+a\lambda^2 te^{-\lambda t}+\int_0^{t}\lambda e^{-\lambda t}g(s)\,ds+\int_t^{\Delta}\lambda^2 te^{-\lambda t}g(s)\,ds,$$

which after transformations becomes

$$\begin{gathered}P^{\Delta}(t)=\frac{\lambda e^{-\lambda t}}{(2\lambda\Delta+3)e^{2\lambda\Delta}+1}\Big((2\lambda\Delta+7)\lambda te^{2\lambda\Delta}+\\ +1-(\lambda t+1)e^{2\lambda t}-2\lambda^2t^2e^{2\lambda\Delta}\Big),\quad t<\Delta.\end{gathered} \tag{49}$$

It can be seen from (48), that ISI distribution $P^{\Delta}(t)$ has δ-function type singularity at $t=\Delta$:

$$P^{\Delta}(t)=\frac{4\lambda\Delta e^{\lambda\Delta}}{(3+2\lambda\Delta)e^{2\lambda\Delta}+1}\delta(t-\Delta),\qquad t\in\left]\Delta-\varepsilon;\Delta+\varepsilon\right[. \tag{50}$$

Consider case B. Here integration in (48) can be performed over the entire domain $]0;\Delta[$ uniformly, which gives

$$P^{\Delta}(t)=e^{-\lambda t}\lambda\int_0^{\Delta} f(s)\,ds=e^{-\lambda t}\lambda,\quad \Delta<t<\tau. \tag{51}$$

Consider case C. Here integration domain should be splitted into two with point $s=t-\tau$, and Eq. (48) turns into the following:

$$P^{\Delta}(t)=\int_0^{t-\tau} e^{-\lambda(s+\tau)}P^0(t-s-\tau)\,g(s)\,ds+e^{-\lambda t}\lambda\int_{t-\tau}^{\Delta} g(s)\,ds+ae^{-\lambda t}\lambda.$$

Here in the first integral $(t-s-\tau)\in[0;t-\tau]\subset[0;\Delta]\subset[0;\tau]$. This allows to identify from Eqs. (4) and (5) exact expression for $P^0(t-s-\tau)$, which is $y_0(t-s-\tau)=e^{-\lambda(t-s-\tau)}\lambda^2(t-s-\tau)$:

$$P^{\Delta}(t)=\int_0^{t-\tau} e^{-\lambda t}\lambda^2(t-s-\tau)\,g(s)\,ds+e^{-\lambda t}\lambda\int_{t-\tau}^{\Delta} g(s)\,ds+ae^{-\lambda t}\lambda.$$

After transformations, one obtains:

$$P^{\Delta}(t)=\frac{\left(K_0+K_1t+K_2t^2+e^{2\lambda(t-\tau)}\right)\lambda e^{-\lambda t}}{(4\lambda\Delta+6)e^{2\lambda\Delta}+2},\qquad \tau<t<\Delta+\tau, \tag{52}$$

where

$$K_0=\left(2\lambda^2\tau^2+4\lambda\tau+4\lambda\Delta+6\right)e^{2\lambda\Delta}-2\lambda\tau+1,$$

$$K_1=\left(2-4e^{2\lambda\Delta}(1+\lambda\tau)\right)\lambda,\quad K_2=2\lambda^2e^{2\lambda\Delta}.$$

Consider case D. Here Eq. (48) turns into the following:

$$P^{\Delta}(t)=ae^{-\lambda(\Delta+\tau)}P^0(t-\Delta-\tau)+\int_0^{\Delta} e^{-\lambda(s+\tau)}P^0(t-s-\tau)\,g(s)\,ds.$$

Let us introduce a new variable of integration, $u=t-s-\tau$:

$$P^{\Delta}(t)=ae^{-\lambda(\Delta+\tau)}P^0(t-\Delta-\tau)+\int_{t-\Delta-\tau}^{t-\tau} e^{-\lambda(t-u)}P^0(u)\,g(t-\tau-u)\,du. \tag{53}$$

From this expression we see, that for calculating the integral one needs to use Eq. (4) either with single, or with two consecutive values of m. Namely, if for some m: $m\tau\le t-\Delta-\tau<t-\tau\le(m+1)\tau$, then one should substitute $y_m(t)$ from (5), corresponding to that m, instead of $P^0(u)$ in the (53). In the opposite situation, there exist such m, that $m\tau<t-\Delta-\tau<(m+1)\tau<t-\tau$. In this case, domain of integration in the Eq. (53) should be split with point $(m+1)\tau$, and as $P^0(u)$ one should substitute either $y_m(t)$, or $y_{m+1}(t)$. Thus, when $t\in[\Delta+\tau;\infty[$, then all possible situations are parameterized with the above mentioned number m in such a way that if $t\in\left[(m+1)\tau+\Delta;(m+2)\tau\right]$, then use $y_m(t)$ from (5), and if $t\in\left](m+2)\tau;\Delta+(m+2)\tau\right[$, then split integration domain and use both $y_m(t)$ and $y_{m+1}(t)$.

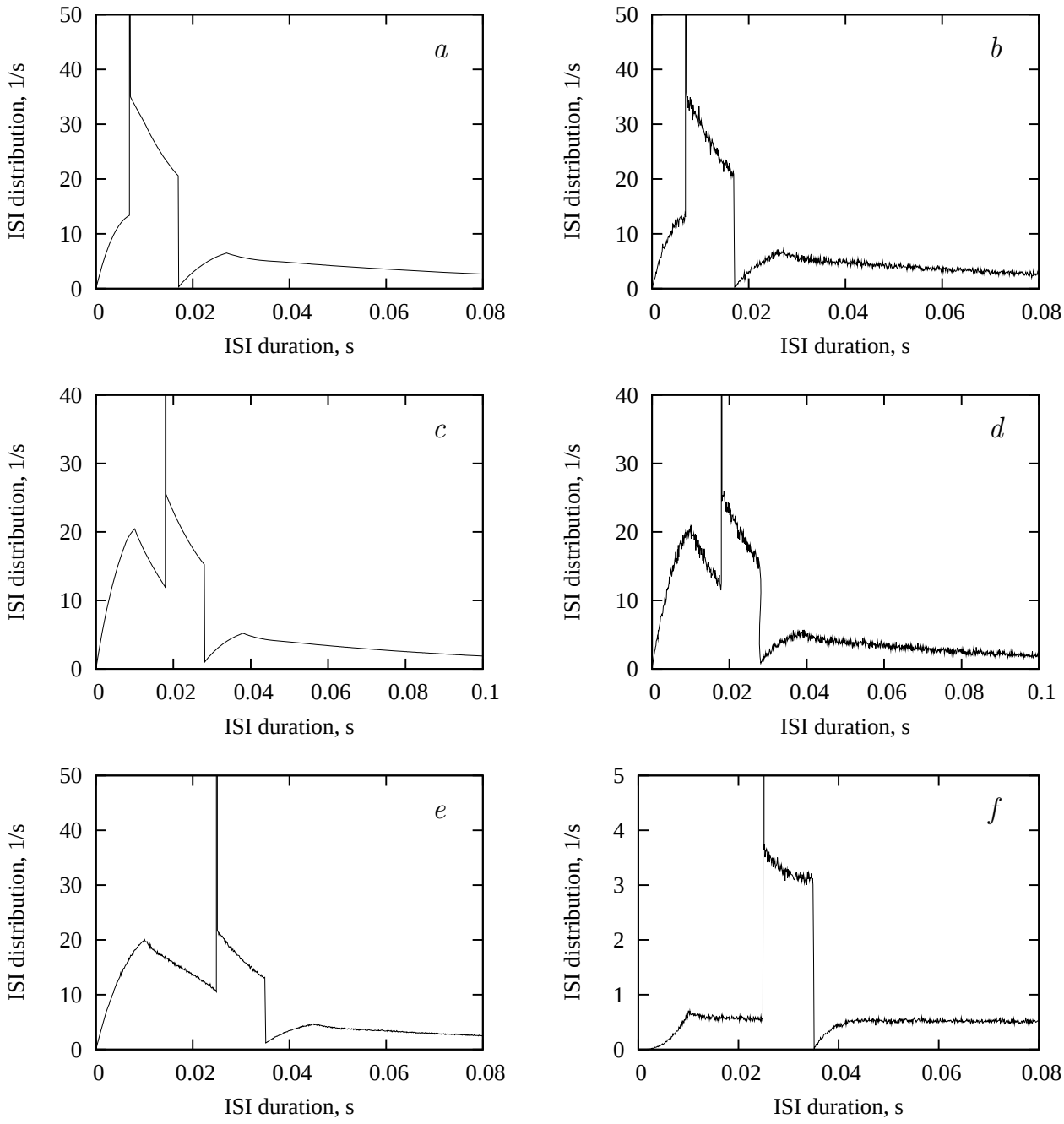

Figure 6. Examples of ISI distribution $P^{\Delta}(t)$, calculated analytically (panels a,c) in accordance with Eqs. (49) – (52), (54), (56) and Eqs. (60) – (64) ; and found numerically, by means of Monte Carlo method (panels b,d,e,f).

a: τ =10 ms, Δ =7 ms, λ =50 s^{-1}, $N_0 = 2$; b: same parameters as in a, 500 000 spikes were produced;

c: τ =10 ms, Δ =18 ms, λ =50 s^{-1}, $N_0 = 2$; d: same parameters as in c, 500 000 spikes were produced;

e: τ =10 ms, Δ =25 ms, λ =50 s^{-1}, $N_0 = 2$, 10 000 000 spikes were produced:

f: τ =10 ms, Δ =25 ms, λ =50 s^{-1}, $N_0 = 4$, 10 000 000 spikes were produced: .

Curves calculated analytically fit perfectly with those found numerically for the same parameters

.

Thus, in the case when there exists such an integer m that $m\tau \le t-\Delta-\tau < t-\tau \le (m+1)\tau$, the integration of (53) gives

$$P^{\Delta}(t) = ae^{-\lambda t}\cdot\sum_{k=1}^{m+1}\frac{\lambda^{k+1}}{k!}\Bigg(\big(t-\Delta-k\tau\big)^{k}+\frac{\lambda}{2(k+1)}\Big(\big(t-k\tau\big)^{k+1}-\big(t-\Delta-k\tau\big)^{k+1}\Big)+$$

$$+\frac{\lambda}{2}\sum_{j=0}^{k}\frac{k!}{(k-j)!\cdot(2\lambda)^{j+1}}\Big(\big(t-k\tau\big)^{k-j}e^{-2\lambda\Delta}-\big(t-\Delta-k\tau\big)^{k-j}\Big)\Bigg)-$$

$$-ae^{-\lambda t}\cdot\sum_{k=1}^{m}\frac{\lambda^{k+1}}{k!}\Bigg(\big(t-\Delta-(k+1)\tau\big)^{k}+\frac{\lambda}{2(k+1)}\Big(\big(t-(k+1)\tau\big)^{k+1}-\big(t-\Delta-(k+1)\tau\big)^{k+1}\Big)+ \quad (54)$$

$$+\frac{\lambda}{2}\sum_{j=0}^{k}\frac{k!}{(k-j)!\cdot(2\lambda)^{j+1}}\Big(\big(t-(k+1)\tau\big)^{k-j}e^{-2\lambda\Delta}-\big(t-\Delta-(k+1)\tau\big)^{k-j}\Big)\Bigg),$$

$$t\in\Big[(m+1)\tau+\Delta;(m+2)\tau\Big].$$

Consider such ISI, that $m\tau < t-\Delta-\tau < (m+1)\tau < t-\tau < (m+2)\tau$, or $t\in\big](m+2)\tau;\Delta+(m+2)\tau\big[$. Taking into account Eqs. (4) and (5), one can rewrite (53) as follows:

$$P^{\Delta}(t)\Big|_{t\in\left](m+2)\tau;\Delta+(m+2)\tau\right[} = ae^{-\lambda(\Delta+\tau)}y_m(t-\Delta-\tau)+$$

$$+\int_{0}^{t-(m+2)\tau}e^{-\lambda(s+\tau)}y_{m+1}(t-s-\tau)\,g(s)\,ds+\int_{t-(m+2)\tau}^{\Delta}e^{-\lambda(s+\tau)}y_m(t-s-\tau)\,g(s)\,ds=$$

$$=ae^{-\lambda(\Delta+\tau)}y_m(t-\Delta-\tau)+\int_{0}^{\Delta}e^{-\lambda(s+\tau)}y_m(t-s-\tau)\,g(s)\,ds+$$

$$+\frac{\lambda^{m+3}}{(m+2)!}e^{-\lambda t}\int_{0}^{t-(m+2)\tau}\big(t-s-(m+2)\tau\big)^{m+2}\,g(s)\,ds-$$

$$-\frac{\lambda^{m+2}}{(m+1)!}e^{-\lambda t}\int_{0}^{t-(m+2)\tau}\big(t-s-(m+2)\tau\big)^{m+1}\,g(s)\,ds=$$

$$=P^{\Delta}(t)\Big|_{t\in\left[\Delta+(m+1)\tau;(m+2)\tau\right]}+\rho_m^{\Delta}(t),$$

where

$$\rho_m^{\Delta}(t)=\frac{\lambda^{m+3}}{(m+2)!}e^{-\lambda t}\int_{0}^{t-(m+2)\tau}\big(t-s-(m+2)\tau\big)^{m+2}\,g(s)\,ds-$$

$$-\frac{\lambda^{m+2}}{(m+1)!}e^{-\lambda t}\int_{0}^{t-(m+2)\tau}\big(t-s-(m+2)\tau\big)^{m+1}\,g(s)\,ds,\quad m=0,1,\ldots \quad (55)$$

Performing integration in (55) one obtains:

$$P^{\Delta}(t)\Big|_{t\in\left](m+2)\tau;\Delta+(m+2)\tau\right[}=P^{\Delta}(t)\Big|_{t\in\left[\Delta+(m+1)\tau;(m+2)\tau\right]}+\rho_m^{\Delta}(t), \quad (56)$$

where

$$\rho_m^{\Delta}(t)=\frac{a\lambda}{2}e^{-\lambda t}\left(\frac{x^{m+3}}{(m+3)!}-\frac{x^{m+2}}{(m+2)!}+\frac{1}{2^{m+3}}e^{-2\lambda\Delta}+\right.$$
$$+e^{-2\lambda\Delta}\sum_{j=0}^{m+1}\frac{x^{m+1-j}}{(m+1-j)!\cdot 2^{j+1}}\left(\frac{x}{m+2-j}-1\right)+ \qquad (57)$$
$$\left.+\frac{1}{2^{m+3}}e^{-2(\lambda\Delta-x)}\right),\quad \text{where}\quad x=\lambda\left(t-(m+2)\tau\right).$$

Note, that in the case $\Delta=0$, ISI distribution for $t\geq\tau$ is completely defined by Eq. (54), which turns into:

$$P^{\Delta=0}(t)=e^{-\lambda\tau}P^0(t-\tau),\quad t\geq\tau. \qquad (58)$$

Eq. (58) coincides with the result for BN with instantaneous feedback, obtained before (see Sec. 'Binding neuron with instantaneous feedback (BNF)' for details).

Graphs of $P^{\Delta}(t)$ for $\Delta<\tau$ are shown at the Fig. 6, a,b.

ISI distribution for $\Delta\geq\tau$

For calculating $P^{\Delta}(t)$ substitute (26) and (27) into Eq. (17). This gives

$$P^{\Delta}(t)=\frac{1}{\lambda}P^0(t)\,f(t)+\int_0^{\Delta}P^{\text{reg}}(t\,|\,s)\,f(s)\,ds. \qquad (59)$$

Further transformation of (59) depends on the domain, t belongs to. Basic domains of t for the case $\Delta>\tau$ are shown in Fig. 4, c.

Consider case A, $t\in]0;\tau]$. Here integration domain, $s\in]0;\Delta]$, should be splitted into two with point $s=t$:

$$P^{\Delta}(t)=\int_0^{t}e^{-\lambda(t-s)}\left(\lambda\Pi(s)-P^0(s)\right)f(s)\,ds+$$
$$+\frac{1}{\lambda}P^0(t)\,g(t)+\int_t^{\Delta}P^0(t)\,f(s)\,ds. \qquad (60)$$

Here Eq. (34) is taken into account.

Consider case B, where $t\in[\tau;\Delta[$. Here integration in (59) should be splitted into three with points $s=t-\tau$ and $s=t$:

$$P^{\Delta}(t)=\int_0^{t-\tau}\frac{1}{\lambda}e^{-\lambda\tau}\left(\lambda\Pi(s)-P^0(s)\right)P^0(t-s-\tau)\,f(s)\,ds+$$
$$+\int_{t-\tau}^{t}e^{-\lambda(t-s)}\left(\lambda\Pi(s)-P^0(s)\right)f(s)\,ds+\frac{1}{\lambda}P^0(t)\,g(t)+\int_t^{\Delta}P^0(t)\,f(s)\,ds. \qquad (61)$$

It can be seen from (59), that ISI distribution $P^{\Delta}(t)$ has δ-function type singularity at $t=\Delta$:

$$P^{\Delta}(t)=\frac{a}{\lambda}P^0(\Delta)\delta(t-\Delta),\quad t\in]\Delta-\varepsilon;\Delta+\varepsilon[. \qquad (62)$$

Consider case C. Here integration domain should be splitted into two with point $s=t-\tau$, and Eq. (59) turns into the following:

$$P^{\Delta}(t)=\int_0^{t-\tau}\frac{1}{\lambda}e^{-\lambda\tau}\left(\lambda\Pi(s)-P^0(s)\right)P^0(t-s-\tau)\,f(s)\,ds+$$
$$+\int_{t-\tau}^{\Delta}e^{-\lambda(t-s)}\left(\lambda\Pi(s)-P^0(s)\right)f(s)\,ds. \qquad (63)$$

Consider case D. Here the intergation in Eq. (59) should be performed over the entire domain $s\in\left]0;\Delta\right]$:

$$P^{\Delta}(t)=\int_0^{\Delta}\frac{1}{\lambda}e^{-\lambda\tau}\left(\lambda\Pi(s)-P^0(s)\right)P^0(t-s-\tau)\,f(s)\,ds. \qquad (64)$$

Integration in (60), (61), (63) and (64) was performed for the simplest case of $\Delta>\tau$, which is $\Delta\in\left[\tau;2\tau\right[$, and the results obtained were used to make graph of $P^{\Delta}(t)$, shown at the Fig. 6, c.

Properties of the distribution

We present here analytical expression and numerical results (see Sec. Numerical Simulations for details), found for statistical characteristics of output stream, namely, for its mean interspike interval, output intensity, second moment of ISI and ISI variation coeffitient. Final analytical expressions are obtained for the simplest case $\Delta<\tau$ for the sake of simlicity.

Mean interspike interval

Let us find mean output ISI, W^{Δ}. Output intensity, λ_o, defined as the mean number of impulses per time unit, is inversed W^{Δ}. The W^{Δ} is defined as:

$$W^{\Delta}=\int_0^{\infty}tP^{\Delta}(t)\,dt.$$

Use here Eq. (17):

$$W^{\Delta}=\int_0^{\infty}tdt\int_0^{\Delta}P^{\Delta}(t\,|\,s)\,f(s)\,ds=\int_0^{\Delta}dsf(s)\int_0^{\infty}tP^{\Delta}(t\,|\,s)\,dt.$$

Use here representation (28), (29) and Eq. (8):

$$W^{\Delta}=\int_0^{\Delta}dsf(s)\left(\int_0^{s}t^2e^{-\lambda t}\lambda^2dt+e^{-\lambda s}\lambda s^2+\int_s^{s+\tau}t\lambda e^{-\lambda t}dt\right)+$$
$$+\int_0^{\Delta}dsf(s)e^{-\lambda(s+\tau)}\int_{s+\tau}^{\infty}tP^0(t-s-\tau)\,dt=$$
$$=\int_0^{\Delta}dsf(s)\frac{2-(1+\lambda s)e^{-\lambda s}-(1+\lambda\tau+\lambda s)e^{-\lambda(s+\tau)}}{\lambda}+$$
$$+\int_0^{\Delta}dsf(s)e^{-\lambda(s+\tau)}\left(s+\tau+\frac{1}{\lambda}\left(2+\frac{1}{e^{\lambda\tau}-1}\right)\right).$$

Use here (34), (44), (45), which gives after transformations:

$$W^{\Delta}=\frac{2\left(\left(2\lambda\Delta+e^{-2\lambda\Delta}+1\right)-2\lambda\Delta e^{-\lambda\tau}\right)}{\lambda\left(2\lambda\Delta+e^{-2\lambda\Delta}+3\right)\left(1-e^{-\lambda\tau}\right)},\qquad \Delta<\tau. \qquad (65)$$

Note, that in the case $\Delta = 0$ Eq. (65) turns into the following:

$$W^{\Delta=0} = \frac{1}{\lambda\left(1-e^{-\lambda\tau}\right)},$$

which coincides with expression obtained before for the ISI first moment of BN with instantaneous feedback (see Eq. (14)).

The output intensity is $\lambda_o^{\Delta} = \frac{1}{W^{\Delta}}$. At large input rates the following relation takes place

$$\lim_{\lambda\to\infty}\left(\lambda_o^{\Delta} - \frac{\lambda}{2}\right) = \frac{1}{2\Delta}. \tag{66}$$

Coefficient of variation

Let's now calculate the coefficient of variation (CV) c_V^{Δ} of output ISI, which is defined as dimentionless dispersion:

$$c_V^{\Delta} \equiv \sqrt{\frac{W_2^{\Delta}}{\left(W^{\Delta}\right)^2} - 1},$$

where W_2^{Δ} is the second moment of output ISI:

$$W_2^{\Delta} \equiv \int_0^{\infty} t^2 P^{\Delta}(t)\,dt = \int_0^{\Delta} ds f(s) \int_0^{\infty} t^2 P^{\Delta}(t \mid s)\,dt.$$

Performing such integration and taking into account Eq. (8), one obtains:

$$\left(c_V^{\Delta}\right)^2 = \frac{-B_1 e^{2\lambda\tau} + 2B_2 e^{\lambda\tau} - B_3}{2\left(\left(2\lambda\Delta + e^{-2\lambda\Delta} + 1\right)e^{\lambda\tau} - 2\lambda\Delta\right)^2} - 1, \tag{67}$$

where

$$\begin{aligned} B_1 = {} & e^{-4\lambda\Delta} - 8e^{-3\lambda\Delta} - 2\left(2\lambda\Delta - 3\right)e^{-2\lambda\Delta} - \\ & -8\left(2\lambda\Delta + 3\right)e^{-\lambda\Delta} - \left(12\lambda^2\Delta^2 + 12\lambda\Delta - 9\right), \end{aligned} \tag{68}$$

$$\begin{aligned} B_2 = {} & \left(\lambda\tau + 2\right)e^{-4\lambda\Delta} - 8e^{-3\lambda\Delta} + 2\left(\lambda^2\Delta\tau - \lambda\Delta + 2\lambda\tau + 6\right)e^{-2\lambda\Delta} - \\ & -8\left(2\lambda\Delta + 3\right)e^{-\lambda\Delta} - \left(12\lambda^2\Delta^2 - 2\lambda^2\Delta\tau + 6\lambda\Delta - 3\lambda\tau - 18\right), \end{aligned} \tag{69}$$

$$\begin{aligned} B_3 = {} & e^{-4\lambda\Delta} - 8e^{-3\lambda\Delta} - 2\left(2\lambda\Delta - 5\right)e^{-2\lambda\Delta} - \\ & -8\left(2\lambda\Delta + 3\right)e^{-\lambda\Delta} - \left(12\lambda^2\Delta^2 + 4\lambda\Delta - 21\right). \end{aligned} \tag{70}$$

The coefficient of variation, given by Eq. (67), depends non-monotonically on the input intensity (see Fig. 7, c).

Theorem 6.

For BN with delayed feedback under Poisson stimulation in the case $N_0 = 2$ *:*

$\forall\tau,\Delta > 0 \;\; \exists\tilde{\lambda} > 0 : \; \lambda \in \left]0;\tilde{\lambda}\right[\Rightarrow c_V^{\Delta} > 1.$

Proof.

Using Eqs. (67)–(70) one easily obtains $c_V^{\Delta}(\lambda,\tau,\Delta)\big|_{\lambda=0}=1$ and $\left(\frac{\partial c_V^{\Delta}}{\partial\lambda}\right)_{\tau,\Delta}\Big|_{\lambda=0}=\Delta+\tau>0$ for $\Delta,\tau>0$, which proves Theorem 6.

Note, that in the case $\Delta=0$ Eq. (67) turns into following:

$$c_V^{\Delta=0}=\sqrt{2\lambda\tau e^{-\lambda\tau}+1},$$

which coincides with expression obtained before for output ISI coefficient of variation of BN with instantaneous feedback (compare with Eq. (16)).

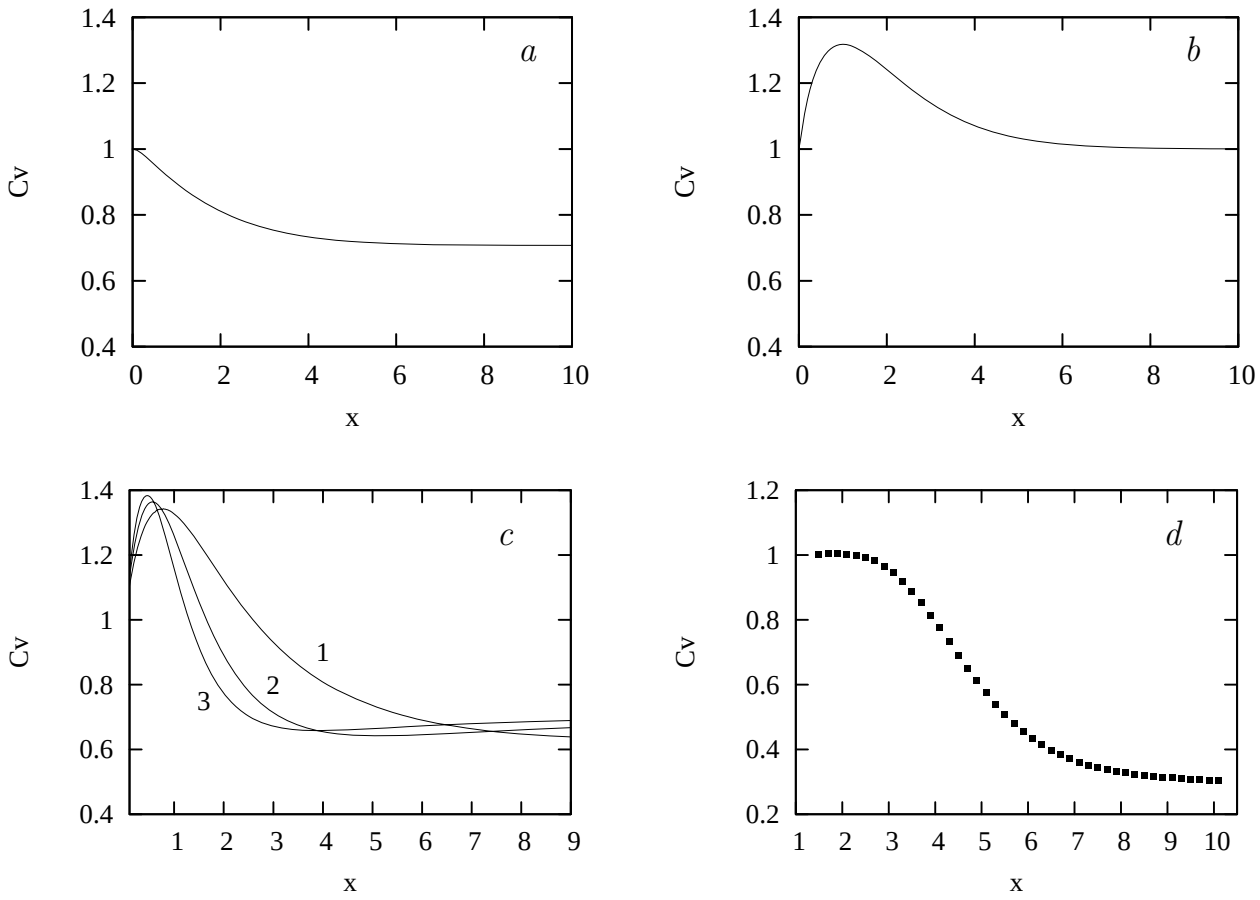

Figure 7. Coefficient of variation as the function of $x=\lambda\tau$:
a: BN without feedback; b: BN with instantaneous feedback; c,d: BN with delayed feedback.
c: CV is found analitically for $N_0=2$, τ =10 ms, Δ =2 ms (1), Δ =5 ms (2), Δ =8 ms (3);
d: CV is obtained numerically for $N_0=10$, τ =20 ms, Δ =8 ms after 50 000 000 triggerings.

NUMERICAL SIMULATIONS

In order to check the correctness of obtained analytical expressions, as well as to get an impression of how do ISI distributions look like for higher thresholds and for the case $\Delta>2\tau$, numerical simulations were performed. A C++ program, containing class, which models the operation manner of BN with

delayed feedback, was developed. Object of this class receives the sequence of pseudorandom numbers with Poisson distribution to its input. The required distribution is achieved by using function ran_exponential() on the uniformly distributed sequence from Mersenne Twister generator from the GNU Scientific Library[ii].

Program contains function, the time engine, which brings system to the moment just before the next input signal, bypassing moments, when neither external Poisson impulse, nor impulse from the feedback line comes. So, only the essential events are accounted. It allows one to make exact calculations faster as compared with the algorithm where time advances gradually by adding small timesteps.

The ISI probability density, $P^{\Delta}(t)$, is found by counting the number of output ISI of different durations and normalization (see Fig. 6, b,d,e,f). In the program, distribution $f(s)$ of time to live of impulse in the feedback line (Fig. 5, b,d,e,f), and the output ISI coefficient of variation, c_V^{Δ} (Fig. 7, d), were calculated as well. Numerically obtained curves fit perfectly with the analytical expressions for $P^{\Delta}(t)$ given in Eqs. (49)—(52), (54), (56) and calculated from (60)—(64), for $f(s)$ given in Eqs. (34), (44), (45) and (46), (47), and for c_V^{Δ} given in (67) – (70).

In order to compare obtained results with those corresponding to other neuronal models, another class, modelling the operating manner of leaky integrate-and-fire (LIF) neuron (Segundo et al., 1968) with delayed feedback, was also included. Namely, the LIF neuron is characterized with the threshold voltage, C, and every input impulse advances by y_0 the LIF membrane voltage, V. Between input impulses the V decays exponentially with time constant τ_M. The LIF neuron fires when V becomes grater or equal C, and $V = 0$ just after firing. Resulting ISI and delays distributions are shown at Fig. 8. Obtained curves are similar to those, found for BN with delayed feedback, see Conclusions and Discussion section for details.

CONCLUSIONS AND DISCUSSION

In this chapter, we derive statistical characteristics of the output stream for single neuron with delayed feedback and present recent results concerning single neuron (Vidybida, 2007) and single neuron with instantaneous feedback (Vidybida, 2008) for comparison. In all cases, neuron is stimulated by the Poisson stream. We use the BN model in order to mimic the operating manner of a biological neuron. This model is an abstract one as it is formulated not in terms of membrane voltage or currents, but in terms of moments when input and output elementary events, which are neuronal impulses (spikes), happen. On the other hand, it is physiologycally grounded as it was inspired by numerical simulation of Hodgkin-Huxley-type neuron (Vidybida, 1996b). The question of how many synaptic impulses in the internal memory are able to trigger the neuron, should be answered on the base of experimental data for real neurons. This number varies from one (Miles, 1990), through fifty (Barbour, 1993), to 60-180 (Andersen, 1991), and 100-300 (Andersen, 1990).

We calculated here ISI probability density functions for binding neuron without feedback, BN with instantaneous and delayed feedback. For BN with threshold 2 ISI distributions are found analytically and numerically, and for higher thresholds – numerically. The obtained functions have remarkable peculiarities which suggest what could happen with spiking statistics of individual neurons in elaborated network with delayed connections.

As we see here, signal processing in BN causes considerable changes in temporal structure of the input signal. Indeed, even in the simplest case of single neuron without feedback the output ISI distribution differs essentially from the Poisson distribution, which is the exponential one.

All ISI distributions, found for BN, BNF and BN with delayed feedback, exhibit derivative discontinuities, see Figs. 3 and 6. Presence of such discontinuities, as well as derivative discontinuity in delays distribution $f(s)$ at $s = \Delta - \tau$ (Fig. 5, c,d,e,f), is due to the finitness of BN's memory, τ.

In the presense of feedback, no matter is it delayed or not, ISI distributions are characterized by breaks, or jumps (see Fig. 3, b and Fig. 6). Such breaks are caused by the discontinuity in the number of impulses from Poisson stream needed for triggering. Namely, when the impulse from the feedback line reaches BN, such number decreases by unity, and increases again when the feedback impulse is forgotten.

In the case of delayed feedback for all considered threshold values output ISI distribution also has δ-function type peculiarity at $t = \Delta$ (see Fig. 6). It can be explained as follows. If the line was empty at the moment of last output spike, impulse enters the line and after time, exactly equal to Δ, reaches BN input. If during time Δ BN receives one impulse from Poisson stream, then the impulse from the line triggers BN exactly through the time Δ after the last spike. Such result is independent from the exact arrival time of Poissonian impulse, therefore, many alternative realizations of driving Poisson process will contribute to its probability. So, the probability to obtain ISI of duration exactly equal to Δ is not infinitesimally small, and ISI distribution exhibits the δ-function type peculiarity at $t = \Delta$.

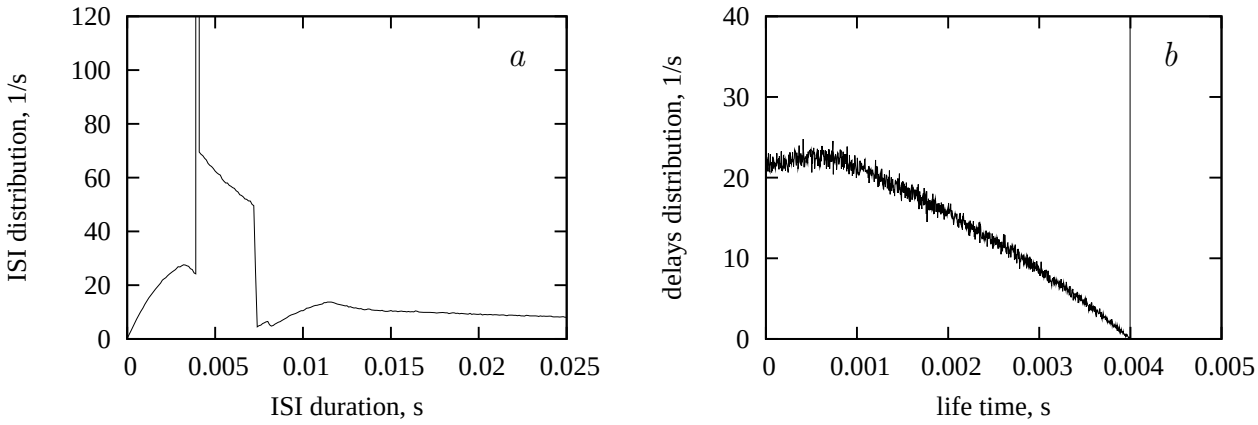

Figure 8. Output stream statistical characteristics for LIF neuron with delayed feedback, C =20 mV, τ_M =3 ms, y_0 =15 mV, λ =100 s^{-1}, Δ =4 ms, obtained numerically after 10 000 000 triggerings: a: ISI distribution $P^{\Delta}(t)$; b: delays distribution $f(s)$.

ISI distributions in the case of delayed feedback, placed on Fig. 6, are polymodal. The shape of ISI distribution and the number of its modes depends essentially on the internal BN's parameters (N_0, τ, Δ), as well as on the input Poisson stream intensity λ.

All mentioned peculiarities were also observed for ISI distributions in the case $\Delta > 2\tau$, obtained in numerical simulations.

For threshold $N_0 = 2$ we also found the mean interspike interval, which is reversed output intensity, as a function of the input one. For high input rates mean output ISI of the BN without feedback will tend to λ / N_0, because almost all input ISIs will become shorter then τ and every consequent N_0 impulses will trigger BN. For the same reasoning, mean output ISI of the BN with instantaneous feedback will tend to $\lambda / (N_0 - 1)$ as $\lambda \to \infty$.

The limiting relation (66), obtained in the case of delayed feedback for $N_0 = 2$, can be understood as follows. At high intensity, every two consecutive input impulses trigger the BN and send impulse into the feedback line, provided it is empty. Thus, output intensity should be $\lambda/2$ plus firing, caused by additional stimulation from the line. This additional stimulation has maximum rate $1/\Delta$, which explaines (66).

Another statistical characteristic of output stream, considered here, was the coefficient of variation. At Fig. 7, a, graph of CV vs. $\lambda\tau$ for $N_0 = 2$ in the case of BN without feedback is placed. It starts from the value $c_V = 1$ and drops motonically to the asymptotic value, $c_V = 1/\sqrt{2}$. It could be explained as follows. At low input rates, when $\lambda\tau \to 0$, BN output stream becomes Poisson. Indeed, the BN will generate the output spike in interval $[t; t+dt[$ if three conditions are satisfied: i) there is input spike in $[t; t+dt[$, ii) the previous input was received at $t-\tau$, or later, iii) the previous input did not trigger BN. Violation of cond. iii), with i), ii) satisfied, is improbable when $\lambda\tau \to 0$. In this case the desired probability of output is $\left(1-e^{-\lambda\tau}\right)\lambda dt$, which describes the Poisson stream with intensity $\left(1-e^{-\lambda\tau}\right)\lambda$. The CV of the Poisson stream equals to 1. Similar reasoning is valid for BNF and for BN with delayed feedback.

Fig. 7, b contains graph of CV vs. $\lambda\tau$ for $N_0 = 2$ in the case of BN with instantaneous feedback. At lower input intensities CV increases with $\lambda\tau$, reaches its maximum at $\lambda\tau = 1$, where mean interval between input impulses from the Poisson stream equals to BN's memory duration τ, and then drops gradually to the asymptotic value, which is 1. There is nothing surprising about that. Indeed, at high input rates, the output stream of BN with instantaneous feedback literally reproduces the input one. So, its CV will coincide with the CV of input Poisson stream, which is 1.

At Fig. 7, c, graphs of CV vs. $\lambda\tau$ for $N_0 = 2$ in the case of delayed feedback at different values of delay Δ are placed. All obtained curves are non-monotonic. For small delay values the maximum is observed near $\lambda\tau = 1$. For higher Δ the maximum position shifts towards lower input intensities, and the highest maximum is observed at $\Delta = \tau$, as it was found in numerical simulations. Obviously, one should expect, that for the case $\Delta \gg \tau$ obtained curve will tend to the shape of CV Graph for BN without feedback, which is monotinically decreasing (Fig. 7, a). Numerical simulations confirm that conclussion.

For high input rates, mentioned dependences stabilize and CV stops to depend on the intensity of input Poisson stream as the rate of lost input impulses tends to zero.

For higher thresholds, the maximum on the CV curve drops, but is always higher then unity. The stabilized CV value also decreases with N_0 increasing, which is crearly understood. Indeed, the variability of the time window, which encloses N_0 input impulses, is smaller for higher N_0. In the case of high input intensity there is almost no lost impulses, so every N_0 consequtive input impulses will trigger BN. If they come in regularly, the output impulsation will also be regular. In the limiting case $N_0 \to \infty$ at high input intensities one should expect output stream to be strictly regular with zero coefficient of variation.

Fig. 7, d, contains CV curve for delayed feedback in the case $N_0 = 10$ for realistic input and output intensities, namely, from 10 to 1000 s^{-1} for the input and from 1 to 100 s^{-1} for the output stream.

The considerable variability of output ISI is consistent with experimental results. High CV values, ranging between 0.5 and 1, were obtained at the output of neurons from primary visual cortex and middle temporal visual area of awake behaving monkey (Softky & Koch, 1993). CV values up to 0.7 were computed from spike trains recorded during spontaneous activity in vivo from neurons in the somatosensory cortex of anesthetized rats (Nawrot et al., 2007) and from primary motor cortex of behaving monkey (Nawrot et al., 2008).

In this work we also wanted to check, wheather the results obtained for BN with feedback, are sensitive to the particular rules, accepted in neuronal model. For this purpose, we performed numerical simulation of leaky integrate-and-fire (LIF) neuron with feedback, driven by the Poisson stream (see Sec. Numerical Simulations). Obtained ISI and delays distributions are placed at the Fig. 8. Obviously, there

exsists remarkable similarity between results, obtained for BN and LIF neuron with delayed feedback, compare Fig. 8, a with Fig. 6; and Fig. 8, b with Fig. 5. Output ISI distributions for LIF neuron with delayed feedback exhibit δ-function type peculiarities, are polymodal, and for some parameters values contain jumps, similar to, and of the same nature as, those observed for BN with delayed feedback. This brings about the idea, that statistical characteristics of the output signal are determined mostly by the network structure (the architecture of its interconnections) and by statistics of the input signal.

On the other hand, we would like to emphasize, that all results, concerning neuron with delayed feedback, are obtained for particular (specific) rules accepted for the feedback line. Namely, at any moment, the line either contains single impulse, or is empty, and it cannot conduct two or more impulses at the same time. And, in our opinion, one should expect similar peculiarities to appear in output firing statistics for any neuronal model with feedback.

Comparing results, obtained for BN and for BN with feedback, we conclude that presence of feedback line can radically change neuronal firing statistics. Moreover, ISI distributions, found for the case $\Delta > 0$, differ essentially as compared to the case of instantaneous feedback. We also expect output ISIs of BN with delayed feedback to be correlated. Indeed, in the case of BN without feedback and BN with instantaneous feedback, at the beginning of every output ISI BN starts from the standard state, which keeps no information about previous events. But the state of BN with delayed feedback is characterized by additional parameter, s, which gets no standard value at the beginning of output ISI and depends on previous events. This, in our opinion, will cause correlations not only between neighbouring output ISI, but also between more distant ones. We expect the output stream of BN with delayed feedback to be non-markovian. Recently, the experimental evidence of correlation between neighbouring ISI from neurons in sensory periphery as well as in cortical neurons was reported (Nawrot et al., 2007; refs. in Farkhooi et al., 2009). The spike trains in electrosensory afferent fibers of the brown ghost knifefish are reported to form a Markov chain of at least fourth order (Ratnam & Nelson, 2000).

REFERENCES

Andersen, P., Raastad, M., Storm, J. F. (1990). Excitatory synaptic integration in hippocampal pyramids and dentate granule cells. In *Cold Spring Harbor Symposia on Quantitative Biology* (pp. 81-86). Cold Spring Harbor: Cold Spring Harbor Laboratory Press.

Andersen, P. (1991). Synaptic integration in hypocampal neurons. In *Fidia Research Foundation Neuroscience Award Lectures* (pp. 51-71). New-York: Raven Press, Ltd.

Barbour, B. (1993). Synaptic currents evoked in Purkinje cells by stimulating individual granule cells. *Neuron*, 11, 759.

Cariani, P. (2001). Temporal codes, timing nets, and music perception. *Journal of New Music Research, 30*, 107-135.

Damasio, A.R. (1989). The brain binds entities and events by multiregional activation from convergence zones. *Neural Computation, 1*, 123-132.

Eckhorn, R., Bauer, R., Jordan, W., Brosch, M., Kruse, W., Munk, M. & Reitboeck, H. J. (1988). Coherent oscillations: a mechanism for feature linking in the visual cortex? *Biological Cybernetics, 60*, 121-130.

Eggemont, J. J. (1991). Rate and synchronization measures of periodicity coding in cat primary auditory cortex. *Hearing Research, 56*, 153-167.

Engel, A.K., König, P., Kreiter, A.K., Gray, C.M. & Singer, W. (1991a). Temporal coding by coherent oscillations as a potential solution to the binding problem: physiological evidence. In Schuster, H.G. & Singer, W. (Ed.), *Nonlinear Dynamics and Neuronal Networks*. VCH Weinheim.

Engel, A.K., König, P. & Singer, W. (1991b). Direct physiological evidence for scene segmentation by temporal coding. *Proceedings of the National Academy of Sciences of the USA*, 88, 9136-9140.

Farkhooi, F., Strube-Bloss, M.F. & Nawrot M.P. (2009). Serial correlation in neural spike trains: Experimental evidence, stochastic modelling, and single neuron variability. *Physical Review E*, 79, 021905.

Feller, W. (1966). *An introduction to probability theory and its applications*, Vol. 2. New York: John Wiley & Sons.

Gerstner, W. & Kistler, W. (2002). *Spiking Neuron Models: Single Neurons, Populations, Plasticity*. Cambridge University Press.

Gnedenko, B. (1989). *The Theory of Probability.* Chelsea (Fifth Edition).

Hebb, D. O. (1949). *The Organization of Behaviour.* New York: Wiley.

Khinchin, A. Ya. (1955). Mathematical methods of mass-service theory. *V. A. Steklov Institute of Mathematics Trudy, 49*, 1-122.

Kistler, W.M., De Zeeuw, C.I. (2002). Dynamical working memory and timed responses: the role of reverberating loops in the olivo-cerebellar system. *Neural Computation*, 14, 2597–2626.

König, P., Engel, A. K. & Singer, W. (1996). Integrator or coincidence detector? The role of the cortical neuron revisited. *Trends in Neurosciences*, 19, 130-137.

König, P. & Krüger, N. (2006). Symbols as self-emergent entities in an optimization process of feature extraction and predictions. *Biological Cybernetics, 94*, 325-334.

Leonards, U., Singer, W. & Fahle, M. (1996). The influence of temporal phase differences on texture segmentation. *Vision Research*, 36, 17, 2689-2697.

Llinás, R., Ribary, U., Joliot, M. & Wang, X.-J. (1994). Content and Context in Temporal Thalamocortical Binding. In Buzsáki, G., Llinás, R., Singer, W., Berthoz, A. & Christen, Y. (Ed.), *Temporal Coding in the Brain* (pp. 251-272). Berlin: Springer-Verlag.

Miles, R. (1990). Synaptic excitation of inhibitory cells by single CA3 hyppocampal pyramidal cells of the guinea-pig *in vitro*. *Journal of Physiology*, 428, 61.

MacKay, D. M. (1962). Self-organization in the time domain. In Yovitts, M. C., Jacobi, G. T. & Goldstein G. D. (Ed.), *Self-Organizing Systems* (pp. 37-48). Washington: Spartan Books.

MacLeod, K., Bäcker, A. & Laurent, G. (1998). Who reads temporal information contained across synchronized and oscillatory spike trains? *Nature, 395*, 693-698.

Nawrot, M.P., Boucsein, C., Rodriguez-Molina, V., Aertsen, A., Grün, S. & Rotter, S. (2007). Serial interval statistics of spontaneous activity in cortical neurons *in vivo* and *in vitro*. *Neurocomputing*, 70, 1717-1722.

Nawrot, M.P., Boucsein, C., Rodriguez-Molina, V., Riehle, A., Aertsen, A. & Rotter, S. (2008). Measurement of variabiility dynamics in cortical spike trains. *Journal of Neuroscience Methods*, 169, 374-390.

Ratnam, R. & Nelson, M.E. (2000). Nonrenewal Statistics of Electrosensory Afferent Spike Trains: Implications for the Detection of Weak Sensory Signals. *The Journal of Neuroscience*, 20, 17, 672–6683.

Rudolph, M. & Destexhe, A. (2003). Tuning neocortical pyramidal neurons between integrators and coincidence detectors. *Journal of Computational Neuroscience, 14*, 239-251.

Segundo, J. P., Perkel, D., Wyman, H., Hegstad, H. & Moore, G. P. (1968). Input-output relations in computer-simulated nerve cell. *Kybernetic, 4*, 157-171.

Smith, G. D. (2002). Modeling the Stochastic Gating of Ion Channels. In Fall, Ch. P., Marland, E. S., Wagnerand, J. M. & Tyson, J.J. (Ed.), *Computational Cell Biology* (pp. 285-319). Singapore: Springer.

Softky, W. R. & Koch, C. (1993). The highly irregular firing of cortical cells is inconsistent with temporal integration of random EPSPs. *Journal of Neuroscience, 13*, 334-350.

Vidybida, A.K. (1996a). Information processing in a pyramidal-type neuron. In Heinz, G. (Ed.), *BioNet'96 – Biologieorientierte Informatik und pulspropagierende Netze, 3-d Workshop* (pp. 96-99), Berlin: GFaI.

Vidybida, A. K. (1996b). Neuron as time coherence discriminator. *Biological Cybernetics, 74*, 539-544.

Vidybida, A. K. (1998). Inhibition as binding controller at the single neuron level. *BioSystems, 48*, 263-267.

Vidybida, A. K. (2006). *Stochastic models.* Kyiv: NAS of Ukraine.

Vidybida, O. K. (2007). Output stream of a binding neuron. *Ukrainian Mathematical Journal, 59 (12)*, 1819-1839.

Vidibida, A. K. (2008). Output stream of binding neuron with instantaneous feedback. *European Physical Journal B, 65*, 577-584.

ADDITIONAL READING

Aroniadou-Anderjaska, V., Ennis, M. & Shipley, M.T. (1999). Dendrodendritic recurrent excitation in mitral cells of the rat olfactory bulb. *Journal of Neurophysiology, 82*, 489-494.

Britvina, T. & Eggermont, J.J. (2006). A Markov model for interspike interval distributions of auditory cortical neurons that do not show periodic firings, *Biological Cybernetics, 96*, 245-264.

Damasio, A.R. (1990). Category-related recognition defects as a clue to the neural substrates of knowledge. *Trends in Neurosciences, 13*, 95-98.

Damasio, H., Grabowski, T. J., Tranel, D., Hichwa, R. D. & Damasio, A. R. (1996). A neural basis for lexical retrieval. *Nature, 380*, 499-505.

Dayan, P. & Abbott, L.F. (2001). *Theoretical Neuroscience: computational and mathematical modelling of neural systems*. Cambridge, Mass: The MIT press.

Fall, Ch.P, Marland, E.S., Wagnerand, J.M. & Tyson, J.J. (Ed.) (2002). *Computational Cell Biology*. Singapore: Springer.

Gray, C.M., König, P., Engel, A.K. & Singer, W. (1990). Synchronization of oscillatory responses in visual cortex: a plausible mechanism for scene segmentation. In Haken, H. & Stadler, M (Ed.), *Synergetics of Cognition*. Berlin: Springer.

Haken, H. (1983). *Advanced Synergetics.* Berlin: Springer.

Haken, H. (Ed.). (1988). *Proceedings of the International Symposium of Schloß Elmau, Bavaria, June 13-17. Neural and Synergetic Computers*. Berlin: Springer-Verlag.

Haken, H. (1996). *Principles of Brain Functioning. A Synergetic Approach to Brain Activity, Behavior, and Cognition.* Berlin: Springer.

Haken, H. (2000). Effect of delay on phase locking in a pulse coupled neural network. *European Physical Journal B, 18*, 545-550.

Haken, H. (2008). *Brain Dynamics. An Introduction to Models and Simulations.* Berlin: Springer.

Hodgkin, A.L. & Huxley, A.F. (1952). A quantitative description of membrane current and its application to conduction and excitation in nerve, *Journal of Physiology, 125*, 221-224.

Holden, A.V. (1976). Models of the stochastic activity of neurons. *Lecture Notes in Biomathematics, 12*, Berlin: Springer.

Keener, J. & Snyde, J. (1998). *Mathematical physiology*. New York: Springer.

Kolmogoroff, A. (1931). Über die analytischen Methoden in der Wahrscheinlichkeit-srechnung. *Mathematische Annalen 104*, 415-458.

MacKay, D.M. (1954). On comparing the brain with machines. *American Scientist, 42*, 261-268.

MacKay, D.M. (1965). From mechanism to mind. In J. R. Smythies (ed.), *Brain and mind: Modern concepts of the nature of mind* (pp. 163-200; 129-131, etc. discussions). London: Routledge & Kegan Paul.

MacKay, D.M. (1980). Neural communication and control: Facts and theories. *Nature, 287*, 389-390.

Matsumoto, M. & Nishimura, T. (1998). Mersenne twister: a 623-dimensionally equidistributed uniform pseudorandom number generator, *ACM: Transactions on Modelling and Computer Simulation. 8*, 3-30.

Moore, B. C. J. (2003). Coding of sounds in the auditory system and its relevance to signal processing and coding in cochlear implants. *Otology & Neurotology, 24*, 243-254.

Nicoll, R.A. & Jahr, C.E. (1982). Self-excitation of olfactory bulb neurones, *Nature, 296*, 441-444.

Nicolls, J.G., Martin, A.R., Wallace, B.G. & Fuchs, P.A. (2001). *From Neuron to Brain*, 4th Ed. Sunderland, Mass: Sinauer.

Schmidt, R. (1975). *Fundamentals of Neurophysiology.* Berlin: Springer.

Scott, A. (2002). *Neuroscience: a mathematical primer*. New York: Springer-Verlag.

Tuckwell, H.C. (1988). *Introduction to theoretical neurobiology.* Cambridge: Cambridge University Press.

Tuckwell, H.C. (1989). *Stochastic processes in the neuro sciences.* Philadelphia: Society for Industrial and Applied Mathematics.

Vidybida, A. K. (2007). Input-output relations in binding neuron. *BioSystems, 89*, 160-165.

Yovitts, M.C., Jacobi, G.T. & Goldstein, G.D. (Ed.) (1962). *Self-Organizing Systems.* Washington: Spartan Books.

KEY TERMS & DEFINITIONS

Neuron: primary constructive unit of neural network. Neuron, either in biological network, like brain, or in tehnical/model network, has integrative function. Namely, it receives input signals from many sources through many input lines, and sends output signals through single output line. In biological neuronal cell, the input lines are named dendrites, and the output line is named axon. The difference between neuron and standard AND/OR logical units used in computers is its manner of taking decision about what output signal should be, based on received input signals. First, a logical unit operates in synchronous manner - all input signal are received simultaneously, while neuron receives signals dispersed in time. Second, a logical unit takes decision about its output based on exact content of signals received, while neuron additionally takes into account the moments the different inputs are received. For this purpose, a neuron must have an internal memory, which keeps for a period of time information about any received signal. In biological neurons, such internal memory is realized as electrochemical transient known as "excitatory postsynaptic potential", or EPSP.

Spike, or action potential: universal electrical signal of neural network, neural impulse. Spikes propagate along the neuron from the place, they started, to the junction with the next neuron. Physiologically spikes are realized through the fast changes of transmembrane voltage due to the ion motion through the ion-channels.

Stochastic process: a process of changing states by a system, in which a state at time t is not determined uniquelly, but can be any state x from some set X of states with some probability $p(x,t)$. The development in time of such a system cannot be predicted as a single trajectory $x(t)$, but can be described by a set of possible trajectories, each with its own probability.

Probability distribution function: Stochastic process can be characterized by a set of multidimentional probability distribution functions[iii] $f(x_n,t_n;x_{n-1},t_{n-1};\ldots;x_1,t_1)$, which gives the probability that stochastic process has states $x_1,\ldots,x_n$ at moments $t_1,\ldots,t_n$, respectively.

Conditional probability distribution function: The function $f\left(x_{n+m},t_{n+m};\ldots;x_{n+1},t_{n+1}\mid x_n,t_n;x_{n-1},t_{n-1};\ldots;x_1,t_1\right)$, where $t_1<t_2<\ldots<t_n<t_{n+1}<\ldots<t_{n+m}$. This function gives the probability, that stochastic process passes states $x_{n+1},\ldots,x_{n+m}$ at moments $t_{n+1},\ldots,t_{n+m}$, respectively, provided that it passed states $x_1,\ldots,x_n$ at moments $t_1,\ldots,t_n$, respectively.

Markovian stochastic process: stochastic process, which has conditional probability distribution functions satisfying the following relation: $\forall n,m\in\mathbb{N},\ t_1<t_2<\ldots<t_n<t_{n+1}<\ldots<t_{n+m}$

$$f\left(x_{n+m},t_{n+m};\ldots;x_{n+1},t_{n+1}\mid x_n,t_n;\ldots;x_1,t_1\right)=f\left(x_{n+m},t_{n+m};\ldots;x_{n+1},t_{n+1}\mid x_n,t_n\right).$$

Poisson process: stochastic markovian process, which states are nonnegative integers n. The process is characterized with intensity λ, and has simplest conditional probability distribution functions of the form $p\left(n,t\mid n',t'\right)=e^{-\lambda\left(t-t'\right)}\dfrac{\left(\lambda\left(t-t'\right)\right)^{n-n'}}{\left(n-n'\right)!}$. All other probability distributions can be found as combinations of the simplest ones based on markovian property.

---

[i] It is worth noticing, that both sorts of variability ogirinate from the variability of driving Poisson process.

[ii] http://www.gnu.org/software/gsl/.

[iii] In pure mathematical literature, the term “probability density distribution” is used.